

Different synthetic approaches, designs and applications of metal-organic frameworks with selected organic ligands

Ubaidullah Hj. Mat Yassin¹, Malai Haniti Sheikh Abdul Hamid¹, Zainab Ngaini² and Ai Ling Tan^{1*}

¹Chemical Sciences Programme, Faculty of Science, Universiti Brunei Darussalam,
Jalan Tungku Link, BE 1410, Brunei Darussalam

²Faculty of Resource Science and Technology, Universiti Malaysia Sarawak,
Kota Samarahan, 94300, Malaysia

*corresponding author email: ailing.tan@ubd.edu.bn

Abstract

Metal-organic frameworks (MOFs) bearing organic ligands with various functional groups and substituents give rise to MOFs of unique crystal structures and topologies. A number of potential applications have been considered for these materials in a wide array of scientific fields, such as in the adsorption of industrially-relevant gases, as heterogeneous catalysts for various organic reactions, as photoluminescent materials, and as antibacterial agents. This review highlights the utility of selected groups of organic ligands in the assembly of main group metals, transition metals, lanthanides and actinides, to generate MOFs of diverse structures in the solid-state, with special attention paid to ligands bearing the carboxylate-, pyridyl-, ether-, imine (Schiff base) moieties, as well as mechanically interlocked molecules (MIMs).

Index Terms: carboxylate, coordination polymers, mechanically interlocked molecules, metal-organic frameworks, pyridyl, Schiff bases

1. Introduction

Metal-organic frameworks (MOFs) are a class of hybrid compounds, composed of metal nodes and organic/inorganic linkers oriented in such a way as to bridge metal ions to generate multi-dimensional, extended structures. Although this class of hybrid compounds was present long before its reported discovery, it was not until 1995 that the renowned chemist Omar M. Yaghi pioneered and extended the work on these unique compounds, which were later termed coordination polymers.¹ This term was first coined in 1916; however, probing the crystalline structure of coordination polymers by X-ray diffraction was not yet possible and so the term was not widely used at that time. MOFs are a subclass of coordination polymers that possess two- or three-dimensional network structures with large internal surface area, high porosity, and thermal stability, which contribute to their exceptionally low densities. Due to these unique intrinsic properties, such compounds are specifically included in a

recently established field of chemistry, known as reticular chemistry. Reticular chemistry is broadly defined as “*the chemistry that utilizes strong molecular bonds to stitch molecules together*”. However, Yaghi himself defined it as the chemistry that concerns linking molecular units into predetermined structures in a repeated manner, held by strong interactions.² MOFs are constructed from coordination and intermolecular bonds, such as London dispersion forces, π -electron stacking, and hydrogen bonds. By exploiting these bonds, frameworks can be constructed. The nature of the metals and ligands employed plays a big role in assembling MOFs. The metal’s coordination number, oxidation state, geometry and Lewis acidity, and the ligands’ flexibility/rigidity, functional groups, bulkiness and Lewis basicity dictate the structure of the resulting frameworks. MOFs classified under reticular chemistry, are porous and thermally stable.³ The porosity of a MOF is a consequence of the ligand adopting specific coordination

modes and geometry with respect to the metal centres, and the significance of MOFs is mainly related to the presence of these pores. Since their first introduction into the world of materials science, MOFs have received much attention from materials scientists and synthetic chemists alike across the globe. Diverse applications of the synthesized MOFs have been investigated, particularly in catalysis and molecular magnets. Additionally, MOFs are also utilized in light-emitting diodes (LEDs) and sensors, in supercapacitors, heterogeneous catalysis, rechargeable batteries, gas separation and biomedicine as potential drug carriers.⁴

There are generally four classes of MOFs, distinguished according to their dimensions, which are nanoparticles, 1D, 2D, and 3D.² The simplest of these classes is the nanoparticle, which is an infinitesimal-sized particle having a diameter of 1 to 100 nm. Second, 1D MOFs - which can exist as linear chains, zigzags, helices, ladders, and tubes - are arranged in a unidirectional manner, with the possible pores occupied by modest-sized molecules.⁵ The third class is the 2D MOFs, which are monolayer in nature, and have a structural topology resembling sheets or layered structures arranged in stacks due to weak interactions. Fourth, 3D MOFs are highly porous and thermally stable networks, whose frameworks spread in three dimensions as a result of tri-directional coordination bonds. These 3D MOFs are of major interest in the extensive study of MOFs, since the pores can accommodate diverse types of molecules for a variety of purposes. Theoretically, an infinite number of MOFs can be prepared simply by varying the combinations and permutations of the metal nodes and ligands used. Inorganic and organic ligands both play a crucial role in building MOFs with specified intrinsic properties, and often, by incorporating a mixture of different metals or ligands in one pot, MOFs of unprecedented characteristics can be tailored.

2. Methods of MOF synthesis

A variety of MOFs can be synthesized by employing different synthetic approaches, and the choice of method generally influences the nature of the MOF formed. The development of

alternative synthetic routes in place of the conventional heating method has enabled the formation of MOFs with interesting network topologies and porosities. Five main synthetic routes have been explored, and these methods include 1) conventional heating and room temperature synthesis, 2) electrochemical synthesis, 3) microwave-assisted heating synthesis, 4) mechanochemical synthesis, and 5) sonochemical synthesis. The choice of methods determines the reaction time, yield, size and morphology of the particles formed. The different synthetic routes mentioned above are summarized below.

2.1 Conventional method

The term conventional method is typically ascribed to the use of electric heating to drive a chemical reaction at temperatures ranging from below to above the boiling point of the solvent used. Reactions above the boiling point of the solvent are called solvothermal reactions, since they occur at elevated temperatures in a closed vessel, enabling a rise in autogenous pressure within the reaction system. Non-solvothermal, or ubiquitously named 'conventional', reactions occur at temperatures below or at the boiling point of the solvent. Room temperature reactions are also classed under the conventional method. The assembly of MOFs can be accomplished even at room temperature, simply by direct precipitation, and by the layering of reactant solutions, followed by slow diffusion or evaporation of the solvent. The conventional method is a good approach for growing single crystals of compounds that do not precipitate instantaneously upon mixing, or that can be recrystallized. Several previously determined MOFs, such as MOF-5 and MOF-177,^{6,7} have been synthesized at room temperature in order to compare the crystallinity, as well as the thermal and chemical stabilities, of the MOFs formed *via* different methods. The room temperature synthesis of MOF-5 is shown in *Figure 1*.

2.2 Electrochemical method

MOF synthesis by the electrochemical method was initially pursued for the purpose of introducing metal ions *via* anodic dissolution to

the reaction medium without including the anions, since it was beneficial in the context of large-scale manufacturing processes. Additionally, this method permits the process to run continuously with higher solid content as compared to typical reactions. The method has been used for the synthesis of a number of prominent MOFs, such

as HKUST-1⁸ and several Cu- and Zn-carboxylates and imidazolates.⁶ **Figure 2** illustrates the reaction conditions for the synthesis of HKUST-1 *via* the electrochemical method using copper metal plates as the electrodes. The crystal structure of HKUST-1 is shown in **Figure 3**.⁹

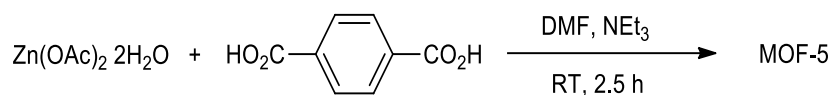


Figure 1. Room temperature synthesis of MOF-5.⁷

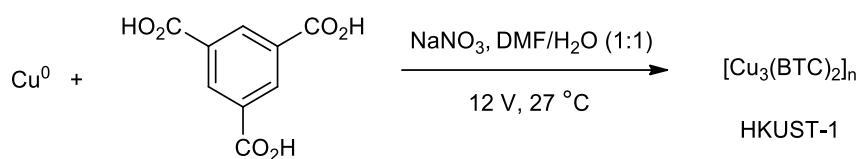


Figure 2. Electrochemical synthesis of HKUST-1.⁸

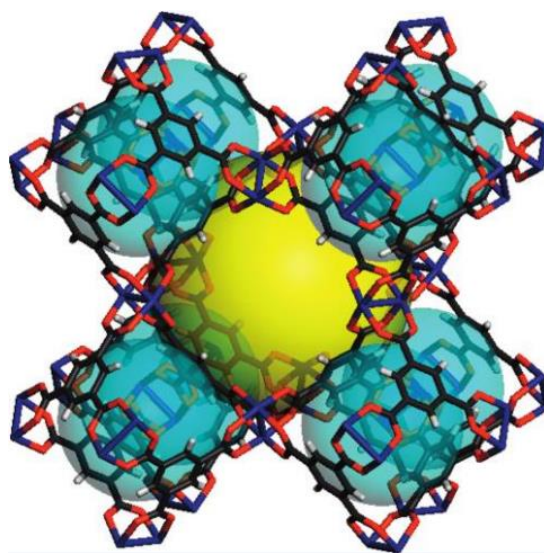


Figure 3. Crystal structure of HKUST-1, depicting the formation of a three-dimensional framework and the presence of major (yellow sphere) and minor (blue spheres) pores. Reproduced with permission from Feldblyum *et al.*⁹ Copyright 2011 American Chemical Society.

2.3 Microwave-assisted synthesis

Synthesis using the microwave-assisted approach is quite a novel method in the field of MOF chemistry, as its utility has been established mainly in organic chemistry. Microwave-assisted synthesis utilizes the coupling interaction between photons in the microwave region of the electromagnetic spectrum and mobile electric

charges. These include metal ions and polar solvent molecules present in the reaction system. Since heating *via* microwave irradiation involves direct interaction between the microwave and the ions or polar molecules (dielectric heating), this method offers a very energy-efficient alternative to the conventional method. The choice of solvent plays a critical role because different solvents

possess different dielectric constants, and thus interact differently with microwave radiation. Similarly to the conventional method, the microwave-assisted method can take place at temperatures below the boiling point of the solvent, as well as under solvothermal conditions.

In MOF chemistry, the microwave-assisted method is commonly employed for the purpose of accelerating the rate of reaction and crystallization of the MOF product, for forming nanosized materials, for improving the purity of the product, for better selectivity, and also for synthesizing desired polymorphs. The past few years have seen a rapid rise in MOF synthesis *via* the microwave-assisted method. Some of these MOFs are Cr-MIL-100, Co-MOF-74¹⁰ and [Ln(Hpmd)(OH)₂] (where Ln³⁺ = Eu³⁺, Gd³⁺ and Tb³⁺; H₄hpmd = 1,4-phenylenebis(methylene)diphosphonic acid).¹¹ The synthesis of Co-MOF-74 using the microwave-assisted method is depicted in **Figure 4**.

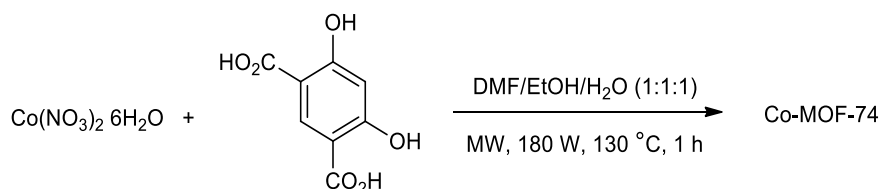


Figure 4. Microwave-assisted synthesis of Co-MOF-74.¹⁰

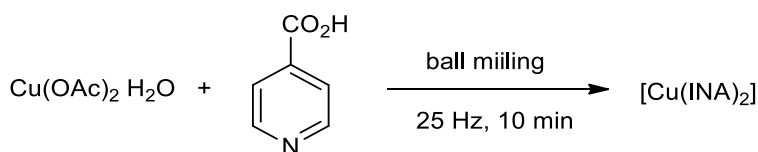


Figure 5. Mechanochemical synthesis of [Cu(INA)₂].¹³

2.4 Sonochemical method

Sonochemical synthesis utilizes high-energy ultrasound to initiate the reaction. Ultrasonic waves generated by the source interact with the liquid medium, forming regions of alternating pressures, which are referred to as compression (high pressure) and rarefaction (low pressure) zones. Since the wavelength of the ultrasonic waves is much longer than the size of the molecules, these waves do not interact directly with the reactant molecular species.

2.4 Mechanochemical method

Mechanochemistry makes use of mechanical force to drive a chemical reaction, which occurs following the dissociation of intramolecular bonds due to mechanical breakage. There are several ways in which mechanochemical synthesis can be carried out, including ball mill grinding, neat grinding, as well as liquid-assisted grinding. The mechanochemical method features a process which is either solvent-free or makes minimal use of solvents, and is considered a green alternative to chemical synthesis. In addition to the neatness of the process, mechanochemical synthesis may prove to be the most suitable method for the bulk preparation of industrially-relevant MOFs, due to the comparatively shorter reaction times needed to obtain high quantitative yields. HKUST-1, MIL-78, MOF-2, MOF-3,¹² and [Cu(INA)₂]¹³ are several examples of MOFs that have been prepared by this method. For example, the mechanochemical synthesis of the MOF [Cu(INA)₂] (where INA = isonicotinate) by ball milling is illustrated in **Figure 5**.

Consequently, cavities are formed, and eventually collapse upon reaching a maximum size. This process leads to the formation of hotspots within the medium that can reach up to 5000 K and 1000 bar for a short time, which is sufficient to drive chemical reactions. Due to its tendency to form nanocrystalline particles, coupled with its environmentally friendly and energy-efficient nature, sonochemical synthesis has been applied for synthesizing many MOF materials, such as IRMOF-9, IRMOF-10, Fe-MIL-53, MOF-5 and

MOF-177.^{6,9} The reaction conditions used in the sonochemical synthesis of MOF-5 are indicated in **Figure 6**.

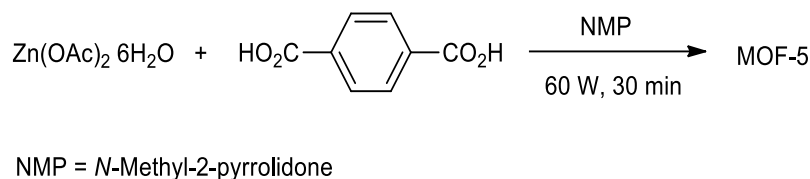


Figure 6. Sonochemical synthesis of MOF-5.¹⁰

3. Linkers in MOF construction

In MOF chemistry, the term *ligand* is often alternatively referred to as a *linker* or *strut*. Organic ligands constitute the majority of the reported MOFs. An array of ligands bearing diverse types of moieties have been introduced as linkers, such as O-, N-, S- and P-based molecules. O- and N-bearing molecules form the majority of the MOF linkers, particularly rigid benzene-*n*-carboxylic acid derivatives, ether and pyridyl derivatives. Additionally, other N-bearing aromatic compounds, *e.g.* pyrazine-containing compounds, Schiff bases, and amines,¹⁴⁻¹⁷ also contribute to a large percentage of the MOFs reported in the literature. The use of sulfonates,¹⁸⁻²⁰ phosphonates,²¹⁻²⁴ and their derivatives as ligands has received attention recently for the diversity of framework structures they form. A group of novel MOFs constructed from complex, highly strained molecules, called mechanically interlocked molecules, have also been reported.²⁵⁻²⁷ Highly stable MOFs based on azolates and mixed donor linkers displaying acid- and base-resistance have also been studied.²⁸ In this review, we summarize the utility of carboxylates, pyridyl and ether derivatives, Schiff bases, as well as mechanically interlocked molecules, as ligands in the assembly of various MOFs (refer to **Table 1**).

3.1 Carboxylate derivatives

The use of rigid *n*-carboxylates as ligands has been well documented in the literature, including di-, tri-, and tetra-carboxylates. A novel cluster-based 3D MOF constructed from the rigid carboxylate ligand 4- (4-carboxyphenyl) -1,2,4 triazole (HCPT) was reported by Zhao *et al.*²⁹ This MOF exhibits two main unique features - the presence

of Ho₈Na and Cu₈I core clusters in a heterometallic framework, as well as its previously unknown 6,12-connected topology. Chang *et al.*³⁰ employed a dicarboxylic acid derivative, 5- (4'-methylphenyl)isophthalic acid, and four N-donor ligands in constructing four low-dimensional Co(II)-based coordination polymers. Another dicarboxylic acid derivative, 3,5-pyridinedicarboxylate (pydc), has also been employed for the synthesis of 1D and 2D Co(II)-MOFs.³¹ The first MOF [Co(pydc)(H₂O)₂]_n consists of honeycomb-like voids, with each of the pydc ligand linked to three Co(II) ions, forming an infinite 2D layer. The second MOF [Co(pydc)(H₂O)₄]_n(H₂O)_n consists of pydc acting as the bidentate ligand, joining two Co(II) ions to give rise to a 1D zigzag chain, with guest water molecules occupying the voids between the polymeric chains. Both MOFs exhibit chemotropism following 2D-1D structural phase transformation upon water exposure, and exhibited reversible phase change between the dehydrated and hydrated forms. Dicarboxylate-MOFs based on lanthanides and actinides have also been studied, such as a series of multifunctional lanthanide-MOFs (Ln-MOFs) from 5-methyl-2-pyrazine carboxylic acid (Hmpca),³² and uranyl-MOFs derived from pyrazine-2,3-dicarboxylic acid (H₂PZDC)³³ and 1,4-naphthalene dicarboxylic acid (H₂NDC)³⁴. The reaction between Ln(NO₃)₃·6H₂O, Hmpca, and K₄[Mo(CN)₈]·H₂O at 1:2:1 molar ratio *via* slow diffusion method yielded photoluminescent Ln-MOFs with a general formula of [Ln(mpca)₂(CH₃OH)₂Ln(H₂O)₆Mo(CN)₈]_n·8H₂O (where Ln³⁺ = Nd³⁺, Eu³⁺, Gd³⁺, Tb³⁺ and Er³⁺).³² The presence of hard base carboxylates, as well as

cyanide as linkers, endowed these permanently porous MOF structures with good thermal stability overall, and efficient emission in the visible region for the Eu(III)- and Tb(III)-MOFs. Hydrothermal synthesis of uranyl-MOFs based on H₂PZDC and H₂NDC generated 1D to 3D MOFs with unique coordination spheres.^{33,34} Different formulae of uranyl-MOFs, such as [UO₂(PZDC)(H₂O)₂], [UO₂(PZDC)(H₂O)] and [(UO₂)₂Cs(PZDC)₂(OH)(H₂O)], were observed upon using NMe₄OH, pyridine, or CsOH as bases, whereas the MOF (H₃O)₂[(UO₂)₂(NDC)₃]·H₂O displayed polycatenation that emerged from the 2D honeycomb grid network established by the H₂NDC ligand. Three MOFs derived from a lactam-dicarboxylate ligand, whose network structures were individually linked by different Mⁿ⁺ ions (where M = Cu²⁺, La³⁺, Pr³⁺), have also been studied.³⁵ Waitschat *et al.*³⁶ utilized hydrothermal treatment for the synthesis of a novel Zr-MOF (CAU-22; where CAU = Christian-Albrechts-Universität) bearing 2,5-pyrazinedicarboxylic acid as the ligand. This hydrophilic MOF comprises hexanuclear clusters of {[Zr₆(μ₃-O)₄(μ₃-OH)₄]} *via* edge-sharing, and offers permanent porosity towards H₂O and N₂. Optimization studies were performed on this MOF using various Zr(IV) salts, as well as by varying the formic acid to H₂O ratio. The authors discovered that optimal conditions for the highest crystallinity MOFs were achieved only when ZrCl₄ and ZrOCl₂ were used in equimolar metal-to-ligand ratio, and at 70:30 and 50:50 formic acid : water ratio, respectively.

The tricarboxylic acid derivative, benzene-1,3,5-tricarboxylic acid (BTC), along with its geometrically similar triazine-cored pyridyl analogue, 2,4,6-tris(4-pyridyl)-1,3,5-triazine (TPT), were exploited in the assembly of Cu(II)- and Ni(II)-MOFs.^{37,38} The Ni(II)-MOF, {[Ni₃(OH)(BTC)₂(TPT)][NH(CH₃)₂]}_n, exists as a two-fold interpenetrated 3D MOF derived from a Ni₃(OH)(COO)₆ trinuclear unit. The combination of these two linkers gave rise to the formation of a new (3,8)-connected 3D net. Similarly, the Cu(II)-MOF with the structural formula [Cu₂(TPT)₂(BTC)Cl]·(solvent)_x, possesses BTC linkers linked to the Cu(II) ions to

form a 2D layered structure, which is further extended by TPT to generate a 3D network. Interestingly, the Cu(II)-MOF exhibits a magnetic long-range ordering at 5 K, demonstrating the strongly frustrated nature of this magnetic MOF.

Tetracarboxylic acid derivatives, such as benzene-1,2,4,5-tetracarboxylic acid (H₄btec), 3,6-dibromobenzene-1,2,4,5-tetracarboxylic acid (H₄dbtec), pyrazine-2,3,5,6-tetracarboxylic acid (H₄pztc), and 2,6-di(2',5'-dicarboxylphenyl)pyridine (H₄L), are known tetratopic linkers for designing MOFs.³⁹⁻⁴¹ Zhang *et al.*⁴¹ reported the synthesis of three isostructural alkali-lanthanide MOFs, with a formula of [K₃Ln₅(pztc)₅(H₂O)₁₉]·7H₂O (where Ln = Dy, Ho, and Yb), derived from H₄pztc. Each of these 3D open frameworks consists of metal ions bridged by the pztc⁴⁻ linkers in a ladder-like square column architecture, whose assembly leads to the formation of an uncommon (4,8)-connected net (refer to **Figure 7**). With the alkaline earth metals Ba(II) and Ca(II), the linkers H₄btec and H₄dbtec yielded pillar-layered 3D MOFs and 3D supramolecular frameworks.³⁹ While the 3D bimodal framework in [Ba₂(dbtec)(H₂O)₂]_n is stabilised by axial Br···π supramolecular interactions, the framework network in [Ca₂(dbtec)(H₂O)₈]_n is held by prominent intra- and intermolecular H-bonding interactions with water ligands. In {[Ba₂(H₂btec)·H₂O]·0.5H₂O}_n and [Ca(H₂btec)·H₂O]_n, a 3D 3-nodal network and a 2D-double layer were observed, respectively. Another interesting study by Siman *et al.*⁴² demonstrated the formation of two rare, porous Na(I)-MOFs based on two tetratopic carboxylate linkers, H₄BDA and H₄BPDA. These Na(I)-MOFs, namely [Na₄(BDA)(CH₃OH)(H₂O)] and [Na₄(BPDA)(H₂O)₂], consist of 2D sodium oxide sheets connected by their respective linkers. Both MOFs crystallize in the monoclinic P2₁ space group with the infinite 2D Na₂O sheets extending in the [010] and [100] directions.

Metal-biomolecule frameworks (MBioFs) have also been designed and synthesized owing to the biocompatibility of the biomolecules incorporated as the organic ligands, such as amino acids, proteins and nucleotides. Imaz *et al.*⁴³ describe the

three main types of amino acid (AA)-based MBioFs. These MBioFs are generally constructed from metal ions with (i) natural AAs; (ii) natural AAs, bridging anions and polydentate ligands; and (iii) chemically-altered natural AAs. Four AA-based MBioFs were synthesized, using the four AAs - aspartic acid (Asp), glutamic acid (Glu), methionine (Met) and histidine (His). These ligands were selected due to their high chelating ability and polydentate nature. Nucleotide- and saccharide-based MBioFs were also crystallographically studied for their potential roles in gas storage, catalysis and biomedicine. Over the past decade, the meticulous exploration of MOFs by the world's leading research groups has had a big impact on the exploitation of MOFs as functional materials. For example, Yaghi and co-workers have been developing complex MOF

systems of unprecedented properties and topologies, by utilizing their profound knowledge of the concept of secondary building units.⁴⁴ One such achievement is in the successful construction of a hierarchical MOF system, known as MOF-500, *via* a one-pot synthetic strategy, comprising a mixed-ligand system - 4,4'-biphenyldicarboxylic acid and 1,2-bis-4-pyridylethane.⁴⁵ An interesting feature of this MOF is its synthetic accessibility using the one-pot approach, which would otherwise be unachievable by stepwise reaction, due to hindrance by the formation of an insoluble intermediate IRMOP-51. In addition, the MOF-500 exhibited a fourfold enhancement of argon sorption capacity, having a specific area of 2274 m² g⁻¹, compared to 544 m² g⁻¹ for its IRMOP-51 precursor.

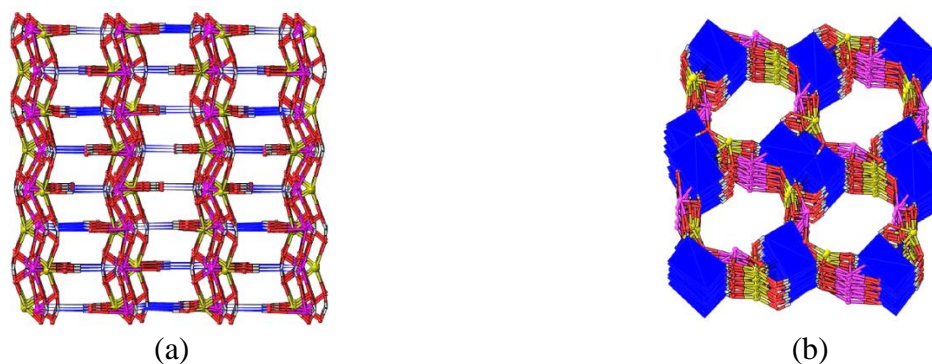


Figure 7. Crystal structure of $[K_5Dy_5(pztc)_5(H_2O)_{19}] \cdot 7H_2O$ as a 3D framework, as viewed (a) along the *c* axis, and (b) along the *b* axis (of the 1D channels).

The pyrazine rings are depicted as planes, and H₂O molecules are excluded for clarity. Reproduced with permission from Zhang *et al.*⁴¹ Copyright 2014 American Chemical Society.

Multivariate (MTV) MOFs, whose structures comprise a number of different organic ligands, were first introduced into the literature by functionalizing MOF-5, and studies on these materials have recently been extended to incorporate mixed metals (*e.g.* MOF-74). MOF-74 is a suitable candidate for expanding the scope of MTV MOFs owing to its infinite rod components linked by 2,5-dioxidoterephthalate ions (**Figure 7**).⁴⁶ Five phase-pure mixed-metal MOFs (each containing 2, 4, 6, 8 and 10 metals per structure) have been successfully synthesized *via* a one-pot solvothermal synthesis.⁴⁷ These MOFs, each abbreviated as MnM-MOF-74 (where *n* = 2, 4, 6, 8 or 10), contain a mixture of

Group II M²⁺ (M = Mg, Ca, Sr, Ba) and divalent transition metal (Mn, Fe, Co, Ni, Zn, Cd) ions. Based on energy-dispersive X-ray spectroscopy and scanning electron microscopy analyses, the crystalline particles of the MOFs were observed to have all metals distributed within their surfaces, with each crystal comprised of a non-linear distribution of the different metals. In one study,⁴⁸ the framework structure of a mechanically unstable Al-based MOF-520, prepared with 1,3,5-benzenetricarboxylate as ligands, was modified with 4,4'-biphenyldicarboxylate (see **Figure 8**), resulting in an exceptional enhancement to its mechanical adaptability, achieved through a process called *retrofitting*. Here, the 4,4'-

biphenyldicarboxylate linkers behave as “girders”, providing a form of mechanical support by linking together two adjacent octametall

SBUs in the MOF. As a result, ultrahigh deformation of the MOF does not occur until the pressure reaches 5.5 GPa.

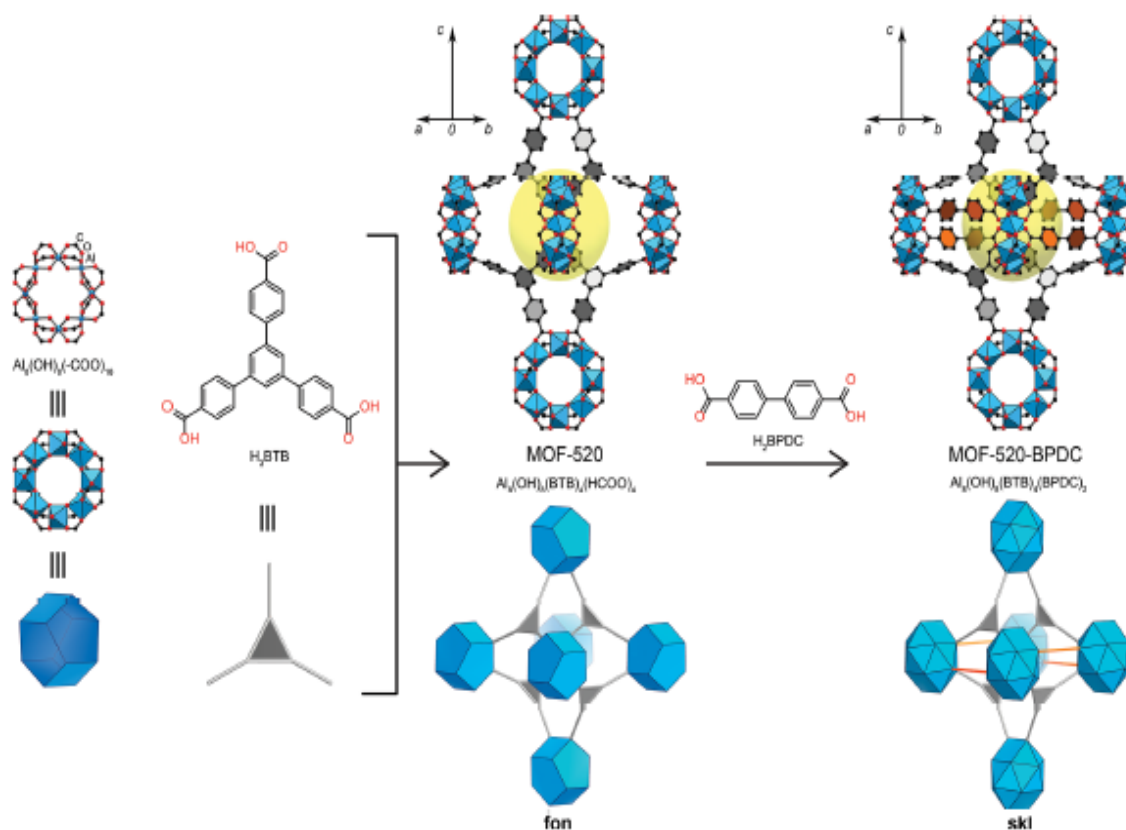


Figure 8. Retrofitting in promoting mechanical stabilisation to MOF-520 via linking two neighbouring SBUs by the 4,4'-biphenyldicarboxylate ligand. The precursor MOF-520 is represented by the dark blue octahedron. Reproduced with permission from Kapustin *et al.*⁴⁸ Copyright 2017 American Chemical Society.

3.2 Pyridyl and ether derivatives

MOFs may be constructed by first preparing discrete units of metalloligands from one metal species at a certain proportion, followed by the addition of ions of the second metal to the solution of former metalloligands. Such an approach was employed previously in the preparation of five mixed-metal organic frameworks (MMOFs) based on two dipyriddy β-diketonates. In their work, Burrows *et al.*⁴⁹ used two analogous ligands, 1,3-di(4-pyridyl)propane-1,3-dione (Hdppd) and 1,3-di(3-pyridyl)propane-1,3-dione (Hdmpdd) to prepare the MMOFs and discovered that the crystal structures of the coordination polymers generated in this way are dictated by the nature of the counteranions used. Two analogous macrocycles prepared from biphenyl - 2,2'-bis(3-pyridylmethylenoxy)-1,1'-biphenylene (3,3'-

bpp) and 2,2'-bis(4-pyridylmethylenoxy)-1,1'-biphenylene (4,4'-bpp) - have been utilized to make MOFs with unusual structural motifs by virtue of the distorted biphenyl spacer.⁵⁰

MOFs with interestingly divergent structural topologies have been constructed from these two macrocyclic ligands with various Zn^{II}, Co^{II}, and Cd^{II} salts as revealed by analyses of their single crystals (**Figure 9**). Although [Zn₂(3,3'-bpp)₂Cl₄] and [Zn₂(3,3'-bpp)₂Br₄] exist as dinuclear metallomacrocycles stabilised by π-π stacking, and [Zn(4,4'-bpp)Cl₂]_n and [Zn(4,4'-bpp)Br₂]_n as 3D structures emerged from the cooperative effects of the 1D polymeric chains, [Co(4,4'-bpp)₂(SCN)₂]_n, [{Cd(4,4'-bpp)₂(SCN)₂}·2H₂O]_n and [Cd(4,4'-bpp)(dca)₂]_n (dca = dicyanamide) on the other hand adopt complex topologies. In the

solid state, $[\text{Co}(4,4'\text{-bpp})_2(\text{SCN})_2]_n$ and $[\{\text{Cd}(4,4'\text{-bpp})_2(\text{SCN})_2\} \cdot 2\text{H}_2\text{O}]_n$ both form 2D polymers, except that $[\text{Co}(4,4'\text{-bpp})_2(\text{SCN})_2]_n$ folds into zigzag chains and rectangular boxes, whereas $[\{\text{Cd}(4,4'\text{-bpp})_2(\text{SCN})_2\} \cdot 2\text{H}_2\text{O}]_n$ consists of interpenetrated layers assembled from alternating left-hand and right-hand cylindrical 2_1 helices. A similar feature was also noted for

$[\text{Cd}(4,4'\text{-bpp})(\text{dca})_2]_n$ as in $[\{\text{Cd}(4,4'\text{-bpp})_2(\text{SCN})_2\} \cdot 2\text{H}_2\text{O}]_n$, but with a formation of 2D Cd^{II} layers made with the coordinating dicyanamide anions. Another Cd^{II} -dipyridyl-MOF displaying reversible adsorption of monohalobenzenes at room temperature has also been reported.⁵¹

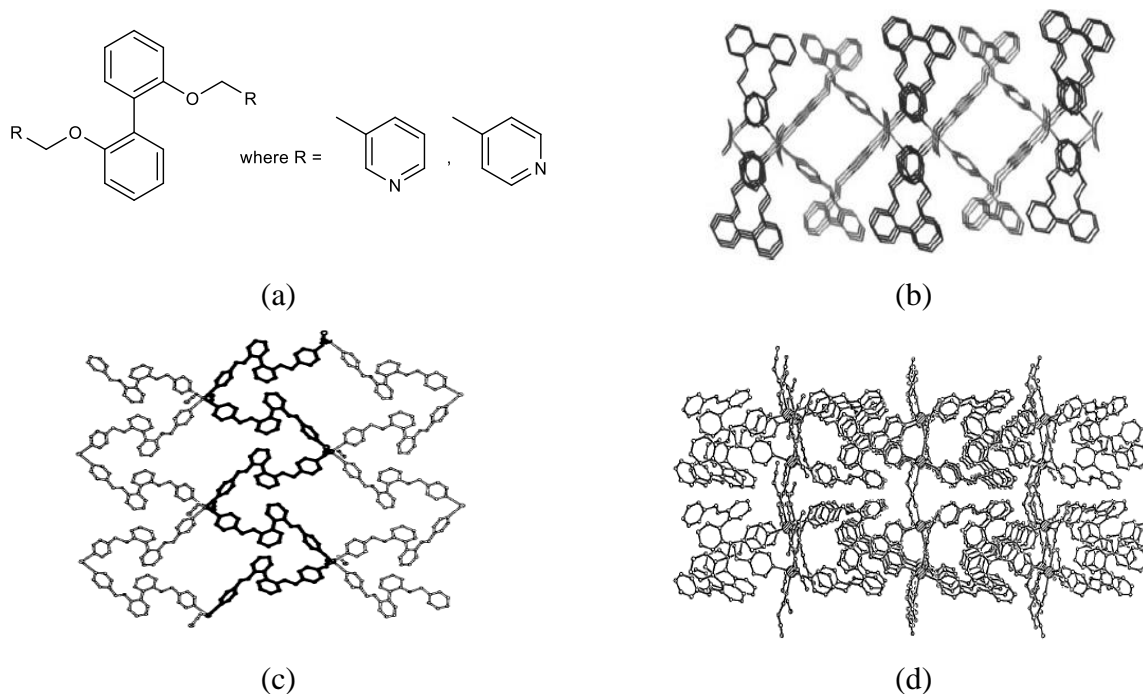


Figure 9. Molecular structure of dipyridyl-based macrocycles used in MOF synthesis as depicted by (a) the crystal structures revealing the packing in (b) $[\text{Co}(4,4'\text{-bpp})_2(\text{SCN})_2]_n$ (along the b axis), (c) $[\{\text{Cd}(4,4'\text{-bpp})_2(\text{SCN})_2\} \cdot 2\text{H}_2\text{O}]_n$ excluding uncoordinated water molecules (along the c axis), and (d) $[\text{Cd}(4,4'\text{-bpp})(\text{dca})_2]_n$ (along the a axis).

Reproduced with permission from Wang *et al.*⁵⁰ Copyright 2004 Wiley-VCH.

The flexible nature of the dipyridyl ligands implies that conformational diversity is anticipated to occur in the MOFs, and as such, can lead to the formation of active sites that are useful as catalytic centres. Liu *et al.*^{52,53} exploited a series of short, isomeric bis(pyridine- n -ylmethoxy)benzene ligands to construct structurally diverse $\text{Cd}(\text{II})$ -MOFs *via* hydrothermal synthesis. By varying the positions of the oxygen atoms on the substituted phenolic rings and those of nitrogen atoms relative to the alkyl chains (either *ortho*-, *meta*-, or *para*-substituted), the topological architecture of the MOFs produced can be diversified. Furthermore, the versatile coordination nature of the Cd^{II} ions can result in different geometries about the metal

centres, as observed in the five MOFs. Three distinct coordination geometries (pyramidal, distorted octahedral, and bipyramidal) were made accessible simply by altering the positions of the donor nitrogen atoms, despite these ligands being positional isomers. Interestingly, these MOFs were discovered to serve as convenient, room temperature photocatalysts for degrading methylene blue, a typical organic dye used in the manufacture of textiles, when irradiated by UV light. Among the five studied MOFs, $[\text{Cd}(1,4\text{-BDC})(\text{bpmp})(\text{H}_2\text{O})_n]$ (1,4-BDC = 1,4-benzenedicarboxylate; bpmp = 1,3-bis(pyridine-3-ylmethoxy)benzene) exhibited the best photocatalytic performance, with a 98.0% degradation ratio of the methylene blue after 120

min. In another study by Wang *et al.*⁵⁴, an ether derivative of benzoic acid, 4,4'-oxybis(benzoic acid) (H₂oba), was exploited in the hydrothermal synthesis of two sodium-lanthanide MOFs based on Eu(III) and Sm(III). The isolated MOFs were isostructural and isomorphous in nature, with a general formula of [NaLn(oba)(ox)(H₂O)] (where Ln³⁺ = Eu³⁺ and Sm³⁺; ox = oxalate). These 3D MOFs consist of distorted tricapped trigonal LnO₉ units, as well as distorted octahedron NaO₆ units, along with the oba and ox ligands. Furthermore, coordination was established by oba and ox ligands to the Ln and Na ions, which generated a 3D network from the 2D inorganic sheets.

Enantiomeric Zn-based MOFs [(*SS*)- and (*RR*)-MOF-1020] having precisely ordered chiral recognition sites have been synthesized *via* the solvothermal method in DMF.⁵⁵ These highly designed MOFs each possess an axially chiral bisbinaphthyl[22]crown-6 moiety as a part of a dicarboxylic acid-terminated ligand (abbreviated as *SS*-2 and *RR*-2). The enantiomeric ligands were prepared by a series of steps, with a terminal reaction involving the palladium(II)-catalysed Suzuki coupling reaction, followed by subsequent hydrolysis of the ester functionality to generate the desired dicarboxylic acid-based ligands. The voids that span the crown ether moiety result in chiral active domains that offer stereoselective recognition of chiral molecules. This feature would permit further development of an array of highly engineered optically active stationary phases to be used in high-performance liquid chromatography, in particular.

A series of pyridyl/triazolyl-MOFs based on Co(II), Cu(II) and Cd(II) ions, and N-heterocyclic auxiliary ligands have been reported by Chen *et al.*⁵⁶ In this work, the authors incorporated camphoric acid to induce racemisation in three of the assembled MOFs under solvothermal conditions. The prepared MOFs adopted a variety of polymeric structures, ranging from a 1D ladder and helical chain, to 3D networks. Among these structures, the three Cd(II)-MOFs, [Cd(SO₄)(4-abpt)(H₂O)]_n·3nH₂O, [Cd(D-cam)(2-PyBIm)(H₂O)]_n, and [Cd(D-cam)(btmb)]_n (where

4-abpt = 4-amino-3,5-bis(4-pyridyl)-1,2,4-triazole; D-H₂cam = D-camphoric acid; 2-PyBIm = 2-(2-pyridyl)benzimidazole; btmb = 1,4-bis(1,2,4-triazol-1-ylmethyl)benzene), exhibited luminescence in the violet region of the visible spectrum, and were second-harmonic generation active, with positive or negative Cotton effects. Their emission spectra displayed similar luminescent behaviour, implying that such an emission originated from ligand-centred emission. In another study,⁵⁷ the ligand 1,2,4,5-tetra(4-pyridyl)benzene (TPB) was exploited for the assembly of a 3D cationic Ag(I)-MOF with the formula of {[AgTPB]·SbF₆]_n. This MOF consists of SbF₆⁻ anions incorporated within its pores, which, upon activation, selectively adsorbs CO₂ and H₂O over CH₄ and EtOH, respectively. A rapid exchange of the dichromate Cr₂O₇²⁻ anion in aqueous media is readily observed at room temperature. The use of MOFs with reactive metal sites bearing Pd-diphosphine pincer complexes has been studied, in the course of which a Zr-MOF was subject to surface modification.⁵⁸ The conversion involved the transformation of the PdI sites, coordinated to a diaminopyridine ligand, into PdBF₄ *via* oxidative I/BF₄⁻ ligand exchange. The modified MOF displayed enhanced selective catalysis towards intramolecular hydroamination involving 2-ethynylaniline over a self-dimerisation process, as well as towards carbonyl-ene cyclisation of citronellal.

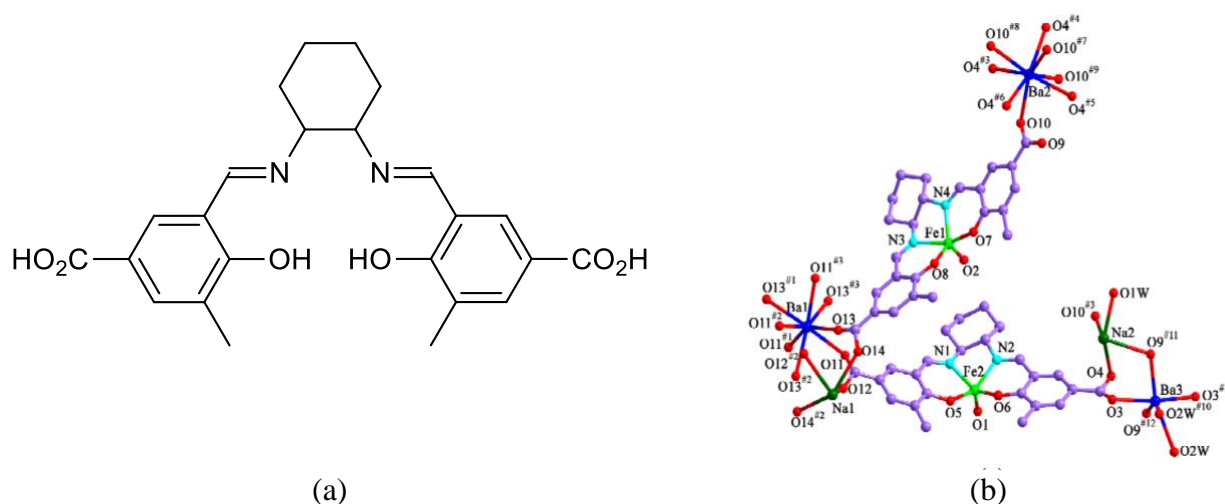
3.3 Schiff bases

Schiff bases are a class of organic compounds that possess the RR¹C=NR² moiety, while those bearing R = H, are specifically known as azomethines (HC=N). They are prepared from the condensation reaction between a carbonyl compound and a primary amine, *via* an S_N2 reaction which proceeds through an iminium intermediate.⁵⁹ Generally, aldehydes react relatively faster with the primary amines, compared to their analogous ketones. Diverse types of Schiff bases have been synthesized, ranging from alkyl to aryl side groups, and from acyclic to cyclic molecules. Schiff bases harbouring aryl functional groups tend to be more kinetically stable than alkyl ones owing to the conjugation of the aromatic ring.⁶⁰ Over the years,

a number of synthetic approaches have been employed for the synthesis of Schiff bases, such as the conventional,⁶¹ mechanochemical⁶² and green⁶³ methods. Conventional synthesis is a common method utilized for Schiff base synthesis. It employs an inert organic solvent, such as methanol, as the reaction medium. The reaction can be performed either at room temperature, or with refluxing at elevated temperatures. The alternative green approach to synthesis has received considerable attention in the field of synthetic chemistry due to its minimal wastage of solvent and also the exclusion of hazardous solvents during the reaction. Schiff bases cover a diverse range of applications in multidisciplinary fields - in medicine as prodrugs⁶⁴ and bioactive compounds,^{65,66} in inorganic chemistry as heterogeneous catalysts⁶⁷, as sensors for heavy metal ions in aqueous media,⁶⁸ as water chain stabilisers in a metal host,⁶⁹ as liquid crystals⁷⁰ and in designing thermo-/photochromic materials.^{71,72}

Alkyl (*e.g.* dichloromethane and chloroform) and aryl halides (*e.g.* bromobenzene) are two classes of closely related halogenated organic compounds that are known to pose detrimental effects (*e.g.* respiratory irritation, liver necrosis) to both

humans and the environment, in general. Thus, synthetic materials that can ‘trap’ these irritant gases are highly sought after, and in recent years, this function has been accomplished by certain porous MOFs. Wang *et al.*⁷³ have reported the first ternary heterometallic organic framework (HMOF) constructed from three metal centres - Fe(III), Ba(II) and Na(I) - and the Schiff base 1,2-cyclohexanediamino-*N,N'*-bis(3-methyl-5-carboxysalicylidene) (see **Figure 10**). This unique HMOF exhibits photocatalytic activity towards the three isomers of chlorophenols (*n*-chlorophenols, *n* = 2, 3 or 4) in the visible region. In another report, a Cd^{II}-MOF based on a novel dipyriddy Schiff base (see **Figure 11**) was synthesized by Xiao *et al.*⁷⁴, revealing selective adsorption of dichloromethane over chloroform under mild conditions (see **Figure 12**). Structurally, this particular MOF comprises two μ -SCN⁻ anions bridging the Cd^{II} centres to generate a rhombus-channeled 3D framework. Each of the Cd^{II} metal nodes possesses a distorted octahedral coordination sphere, in which two N atoms from the ligand, as well as two S and two N atoms from the thiocyanate anions, are coordinated to it. The thiocyanate anions act as the bridging ligands, linking adjacent Cd^{II} metal ions to form a metal-thiocyanate inorganic polymer chain.



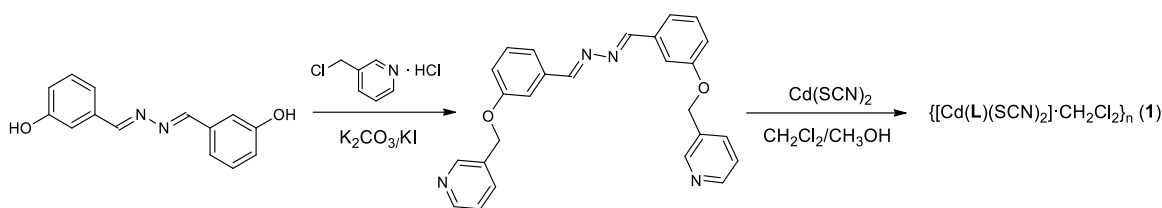


Figure 11. Synthesis of 3-(aryl ether)pyridyl azine derivative and its Cd^{II}-MOF.⁷⁴

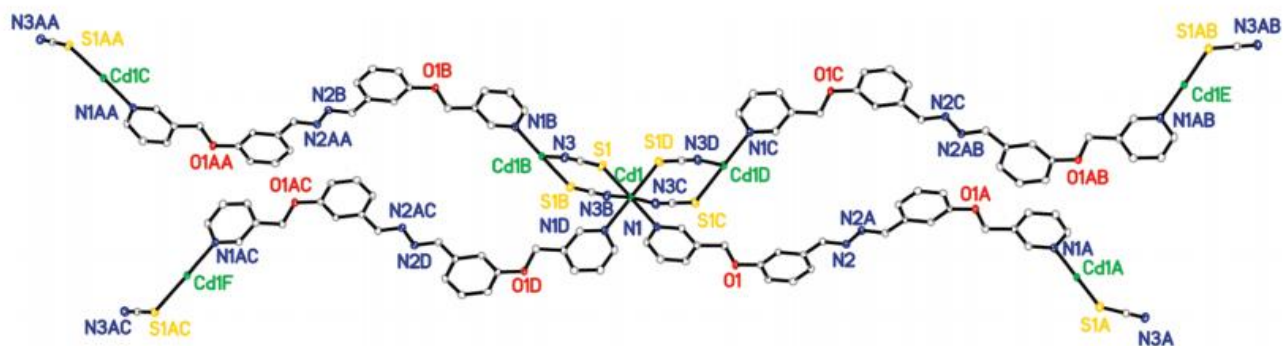


Figure 12. ORTEP representation of the coordination environment of the Cd^{II}-MOF, showing its polymeric chain structure. Reproduced with permission from Xiao *et al.*⁷⁴ Copyright 2011 American Chemical Society.

A highly thermally stable, porous Ag(I)-based MOF, reported by Cheng *et al.*,⁷⁵ and derived from the Schiff base 3,6-bis[2-(4-oxide-quinoxaline-yl)-4,5-diaza-3,5-octadiene], has been shown to effectively isolate benzene from its six-membered organic analogues. Zhang *et al.*⁷⁶ reported the solvothermal synthesis of four 2D network coordination polymers based on Zn(II) and Cd(II). These polymers were found to exhibit greatly enhanced electrochemical luminescence (ECL) with ECL yields of 0.56-0.72. According to the authors, this intensified ECL emission is attributed to the enhanced spin-orbit coupling effect exerted by the incorporation of Zn ions. In another study,⁷⁷ the authors demonstrated the self-assembly of two Co(II)-MOFs, [Co₆(SO₄)₂(BTEC)(OH)₄·3H₂O]_n (1) and [Co₂(BTEC)(4-bpdb)(H₂O)₂·4H₂O]_n (2), under hydrothermal conditions by incorporating a mixture of 1,2,4,5-benzenetetracarboxylic acid (H₄BTEC) and 4,4'-dipyridylamine (dpa) or 1,4-bis(4-pyridyl-2,3-diaza-1,3-butadiene(4-bpdb)). In MOF 1, coordination was achieved by SO₄²⁻ instead of the dpa ligand, owing to steric hindrance imposed by BTEC⁴⁻, which prevents the participation of the shorter length of dpa in the coordination. Another Co(II)-MOF derived from the Schiff base 4,4'-[benzene-1,4-

diylbis(methylylidenenitrilo)]dibenzoic acid (H₂bdda), having an empirical formula of Co₂(bdda)_{1.5}(OAc)·5H₂O (abbreviated as UoB-3), was synthesized ultrasonically at room temperature.⁷⁸ Based on catalytic studies, the authors discovered that UoB-3 showed a good performance as a heterogeneous catalyst for the oxidation of various primary and secondary alcohols (75-95% yields, 65°C, ≤75 min), as well as the Henry reaction (62-88%, 70°C, 24 h). Two asymmetric vanillin-derived Schiff base ligands, namely 4-hydroxy-3-methoxybenzaldehyde nicotinoylhydrazone (L₁) and 4-hydroxy-3-methoxybenzaldehyde salicyloylhydrazone (L₂), were employed for the assembly of five coordination polymers based on Pb^{II}, Cu^{II} and Co^{II}.⁷⁹ A notable feature was observed in the reaction between Pb^{II} salts and L₁ after changing the anion present in the Pb^{II} salt used, namely that the presence of acetate ions in the reaction mixture promotes the formation of a 1D structure with formula Pb₂(L₁)₂(OAc)₂(H₂O)₂, whereas a 3D diamondoid structure [Pb₂(L₁)₂(NO₃)₂]·3H₂O is obtained when a nitrate ion is present (refer to **Figure 13**). Similarly, while the reaction between Co(NO₃)₂ and L₂ in MeOH/CH₂Cl₂ and pyridine favours the formation of a discrete complex with

the formula $[\text{Co}^{2+}(\text{L}_2)_2(\text{py})_2] \cdot 2\text{CH}_3\text{OH} \cdot \text{H}_2\text{O}$, using $\text{Co}(\text{ClO}_4)_2$ instead gives rise to a 1D extended complex structure, namely $[\text{Co}^{3+}(\text{L}_2)_2(\text{py})_2] \cdot \text{ClO}_4$.

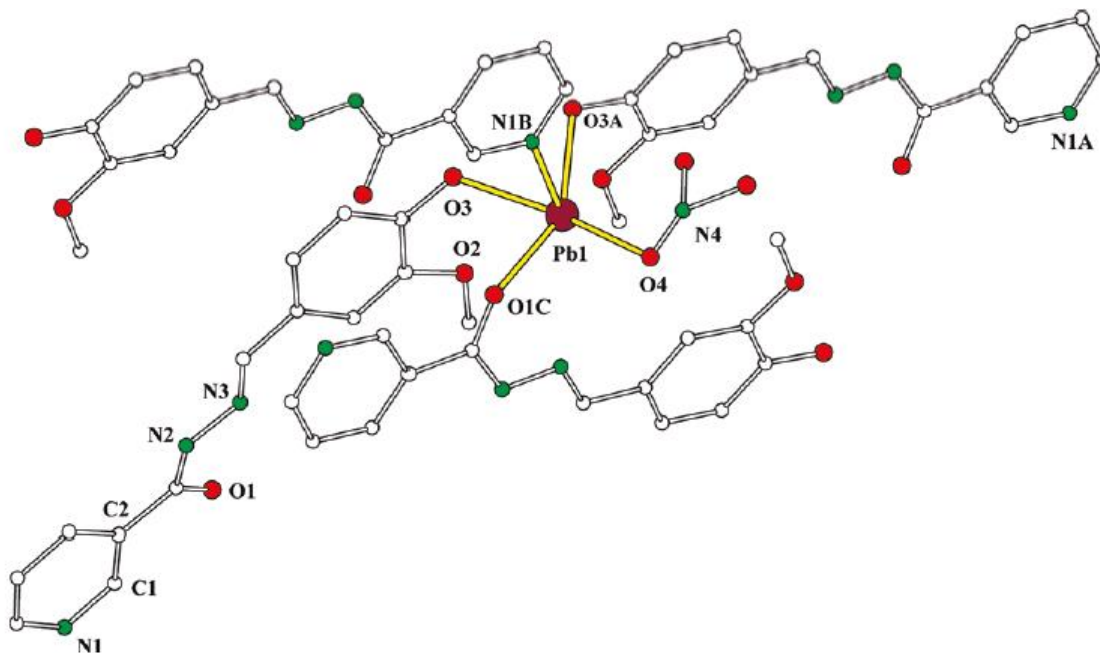


Figure 13. The crystal structure of the polymeric $[\text{Pb}_2(\text{L}_1)_2(\text{NO}_3)_2] \cdot 3\text{H}_2\text{O}$, illustrating the coordination environment around the Pb^{II} ion.

Reproduced with permission from Li *et al.*⁷⁹ Copyright 2010 American Chemical Society.

3.4 Mechanically interlocked molecules

Mechanically interlocked molecules (MIMs) are topologically linked molecules that are not connected by conventional bonds. They consist of two or more organic molecules that are assembled in a stable, ring-like manner, which display interlocked components arranged perpendicular to each other. [2]Rotaxanes, cucurbit[6]uril, dibenzo[24]crown-8 ether wheels, and [2]catenanes are several examples of these intricate MIMs that have been incorporated as MOF linkers.⁸⁰ They are of paramount importance for developing molecular shuttles and switches for functional ultrahigh-density electronics. Interestingly, MIMs in several reported MOFs are the most complicated ligands ever employed in MOF synthesis. In two related reports,^{81,82} two analogous catenane units of MIMs derived from cyclophanes and polyether rings were incorporated into MOFs to give two previously unknown MOFs, namely MOF-1011 and MOF-1030. The shorter and longer MIM ligands recorded remarkable lengths of 19.3 and 32.9 Å, respectively, with the 'linear' part of the ligand

benz as a result of the strain imposed by the vast conjugated π -system. Covalently attaching the MIMs as MOFs enhances the performance of the MIMs by strongly restricting the translational motion of the molecules, since their performance is optimal when highly ordered and coherent. MOF-1011 assembles as a 2D MOF, whose framework consists of trigonal $\text{Cu}(\text{I})$ units and ligand backbones, generating high density layered structures. This accomplishment is another stepping stone in MOF chemistry, since the field of catenane-MOFs is relatively new, and single crystals of catenane-MOFs have not been well studied, as a consequence of the bulkiness and lack of symmetry, coupled with the rigid yet dynamic behaviour of the catenanes.

A Zn-MOF based on a hexacarboxylate-[2]rotaxane MIM linker, with the formula $\{[\text{NH}_2\text{Me}_2]_2[\text{Zn}_2(\text{H}_2\text{O})_2(\text{L})](\text{H}_2\text{O})_{1.25}\}$ ($\text{L} = \text{MIM}$ linker), has been reported by Gholami *et al.*²⁵ The repeating unit of the resulting MOF is made of all six of the carboxylate groups on L coordinated to a Zn ion of a secondary building unit. The six

negative charges on the anionic framework are counterbalanced by two dimethylammonium ions, generated from the thermal decomposition of the DMF solvent during the solvothermal treatment. Each of the two independent Zn centres adopts tetrahedral geometry with the three different carboxylate ends of the linker coordinated to it. Variable-temperature powder X-ray diffraction in a temperature range 25-200 °C revealed that the crystalline structure had been preserved, indicating the robustness of the material owing to the highly restricted motion of the framework. MIMs bearing amide²⁶ and amine²⁷ moieties have also been explored, and utilized in the synthesis of an Ag(I)-isophthalamide [2]catenane, and a Cu(II)-[2]rotaxane MOF, respectively. The Cu(II)-[2]rotaxane MOF has a formula of $[\text{Cu}_2(\text{MIM})(\text{H}_2\text{O})_2] \cdot 3\text{H}_2\text{O}$, adopting an unusual β -phase of NbO topology with lattice water occupancy of 11% in the pores. Interestingly, upon the activation of the Cu(II)-MOF by the removal of the water, the structural integrity of the framework was retained and remained unaffected after a further activation-deactivation process. On the other hand, the Ag(I)-isophthalamide [2]catenane was found to exist as a 1D coordination polymer, with the formula $\{[\text{Ag}(\text{MIM})](\text{OTf})\}$, and the asymmetric unit consists of one catenane molecule, one Ag(I) ion and OTf^- anion, as well as disordered solvent molecules. The pyridine units of the macrocycles from neighbouring catenanes coordinate to the Ag(I) ions, adopting a distorted linear geometry. Further, the 2D lattice formed is stabilised by the π -stacking between the chain dimers.

Several transition metal- and lanthanide-based MOFs bearing MIMs have been studied, including the Texas-sized molecular box (TSMB) MIMs. These TSMB MIMs are essentially [2]pseudorotaxanes linkers designed from tetraimidazolium macrocycle and typical dicarboxylates.⁸⁰ One TSMB, derived from 2,6-naphthalene-dicarboxylate (L^{2-}) formed an Ag(I) MOF with formula $[\text{Ag}_2(\text{L} \subset \text{TSMB})(\text{L})][\text{L}]$ giving rise to a framework structure comprising each Ag(I) centre coordinated to two carboxylate groups in a *trans* geometry, with Ag-Ag distances

of 13.5 and 13.8 Å, as well as the incorporation of non-coordinated charged L and water molecules within the pores. However, for its Zn(II) analogue $[\text{Zn}_2(\text{L} \subset \text{TSMB})(\text{L})_3] \cdot (\text{H}_2\text{O})_6$, the tetrahedral Zn(II) centres are ligated by four carboxylate moieties, forming an interpenetrated diamondoid topology, with the pores occupied by interpenetration from the adjacent framework and water molecules. A 1,4-benzene-dicarboxylate derived TSMB (L^{2-}) was also employed as a ligand for constructing Ln(III)-based MOFs (Ln = Nd, Eu, Sm, and Tb). With Nd(III), a MOF with the formula $[\text{Nd}_2(\text{L} \subset \text{TSMB})_{4.5}(\text{H}_2\text{O})_4(\text{L}2)_{0.5}]$ was obtained, which exists as a poly-cationic three-periodic framework. Meanwhile, neutral three-periodic frameworks with the formula $[\text{M}_2(\text{L} \subset \text{TSMB})(\text{H}_2\text{O})_2(\text{L}2)_4]$ were obtained when M = Eu, Sm, and Tb. In the latter, the axle dicarboxylate linkers of the MIM molecules join the polymer into a 3D structure.

4. Applications of MOFs

MOFs have been studied for their potential applications in a variety of fields, such as catalysis, photoluminescent devices, gas storage and separation, and as antibacterial agents. N-rich ligands (triazines, tetrazoles, and hydrazines) have potential applications as high-energy MOFs.⁸³ Additionally, MOFs bearing superacidic sites useful for Brønsted acid catalysis for various organic transformations also open up a number of new possibilities in catalytic chemistry.⁸⁴ **Table 2** summarizes several applications in which MOFs have been extensively studied.

4.1 MOFs as heterogeneous catalysts

Post-synthetic modifications (PSMs) involve chemically modifying the organic functional groups that form the exterior regions of pores of the MOF surface. These chemically altered sites now exhibit an increase in reactivity that permits the activated surfaces to participate in various chemical or physical processes, such as organic catalysis, electrocatalysis and proton conduction. The activated surfaces provide an enhanced specific surface area for selective catalytic reactions, which are highly dependent on the pore size, as well as the geometry and dimensions of

the potential substrate molecules. MOFs with free amine groups can be easily converted into an azomethine group so that new functionalities can be introduced into the previously short surface ligands for complexation with metals for the desired catalysis.

In one study, an isoreticular MOF (IRMOF-3) was post-synthetically modified to incorporate Au(III) to generate a new Au(III)-based IRMOF, designated as IRMOF-3-SI-Au. The modified version had the highest turnover frequency of 52 h, followed by its Au-Schiff base complex analog, Au/ZrO₂ and AuCl₃, being 40, 12, and 3 h⁻¹, respectively. The unreacted amine group in the IRMOF-3 was initially reacted with salicylaldehyde to form its imine analog, and then followed by complexation with the tetrachloridoaurate(III) ion.⁸⁵ PSM has enabled the design of an efficient catalytic system with the catalytically active molybdenyl acetylacetonate site supported on a UiO-66-NH₂ MOF, effective for the epoxidation of both cyclic and aliphatic alkenes.⁸⁶ In this study, the Schiff bases salicylaldehyde (SA) and thiophene-2-carbaldehyde (TC) were reacted with the free aminated MOF surface, to give SA-Mo and TC-Mo analogs of the same MOF. Meanwhile, hydrogen peroxide, sodium iodate(VII) and *tert*-butyl hydroperoxide (TBHP) were preferentially selected as the oxidants, with TBHP giving the highest epoxide yield of 94% and 97% at the refluxing temperature of 1,2-dichloroethane for the SA-Mo and TC-Mo versions, respectively. In a recent study,⁸⁷ a Pd(II)-pyridylsalicylimine complex was successfully anchored hydrothermally onto the voids of a MOF, Cu(BDC), resulting in efficient, better recyclability, and a more selective catalyst for the Mizoroki-Heck coupling reaction.

4.2 MOFs as photoactive devices

Similar to discrete metal complexes, hybrid compounds such as MOFs have been studied for their potential utility as sensing devices due to their photoluminescent properties. Matthes *et al.*⁸⁸ have utilized the solvent-free synthetic strategy to construct intralanthanide MOFs, comprising Eu³⁺, Tb³⁺, and Gd³⁺ at various ratios with 4,4-

bipyridine as the linkers, for the purpose of tuning the emission colour of the resultant MOFs. Since Eu³⁺, Tb³⁺ and Gd³⁺ have statistically identical ionic radii (115, 112, 114 pm, respectively, when the coordination number = 7) as well as close proximity in both chemical characteristics and oxidation states, such a mixed crystal can be experimentally accomplished. Emission colours of red, orange, yellow and green were generated simply by varying the relative ratios of the lanthanides. Pure Eu³⁺ and Tb³⁺ ions have characteristic emissions in the red ($\lambda = 702$ nm) and green ($\lambda = 488, 546$ nm) regions, respectively. By mixing the two ions in selected proportions, different emission colours and intensities can be produced. Interestingly, the incorporation of Gd³⁺ into the framework only effectively mitigated the number of luminescence centres by quenching, and did not directly participate in the tuning process. In addition, the N₂ sorption behaviour of these lanthanide MOFs was investigated, and it was discovered that they possess microporosity as well as mesoporosity in the range 0.6-1.8 nm, with a maximum adsorptivity of 172 cm³ g⁻¹ at 315 °C, and a BET surface area of 660 m² g⁻¹.

Among the critical factors for the successful construction of MOFs (such as the method of synthesis, nature of the solvent used, reaction time and temperature, nature of anions present, pH and concentration of the starting materials, coordination numbers of the metal ions, as well as the flexibility or rigidity of the organic ligands used), the metal to ligand (M:L) molar ratio has been widely investigated, as it has been demonstrated that beyond a particular ratio the framework disintegrates and forms individual metal complexes instead.⁸⁹ A novel, rigid, dumbbell-shaped ditopic (two binding pockets) pybox ligand with six potential coordinating atoms formed a highly emissive coordination polymer with Eu(III) ions as the metal nodes. Absorbance measurements under Job plot conditions revealed that the optimum M:L ratio for MOF formation was 1.5:1, which was also correctly predicted based on the fact that Eu(III) possesses a maximum coordination number of 9, and the pybox ligand is 6-coordinating in nature, and thus $9/6 = 1.5/1$. Importantly, this Eu(III)-

based coordination polymer's dynamic behaviour in solution against other lanthanides (Tb(III) and Sm(III)) has been investigated, in addition to spectroscopic analyses that revealed the observed intense red emission, with remarkable quantum yields reaching up to 73%. These two properties of the coordination polymer would enable its equipment in photomaterials, and also in polymetallic emitting materials.

Beziau *et al.*⁹⁰ utilized α,β -unsubstituted dipyrin ligands (dpm) for the construction of a series of Cd(II) complexes with a general formula of [Cd(dpm)₂]. Among these complexes, complex 5 exists as a discrete structure in a tetrahedral environment, while complexes 7·MeOH, 7, and 8 form 1D, 2D and 3D coordination polymers, -9 were obtained as the cis-9 and trans-9, each consisting of Cd(II) centres chelated by two dpm ligands and two monodentate pyridine ligands, existing in the octahedral coordination geometry. Although solid-state luminescence studies revealed the quantum yield to be less than 1%, these Cd(II) complexes were the first series of crystalline coordination polymers bearing mono-dpm as ligands reported to possess luminescence behaviour.

4.3 Liquid and gas storage and separation

MOFs have been thoroughly explored for their practical utility in adsorption of industrially relevant liquids and gases, particularly H₂, which has been a challenge due to its lower density than air, and its inherently explosive nature. In addition, MOFs offer liquid and gas separation as well as storage that can be achieved by engineering the van der Waals radius or diameter of the open cavities. Pores, voids, or cavities play a pivotal role enabling entrapment of molecules of specific dimensions (termed guest molecules), and may possess catalytic sites. These guest molecules can be exposed to the unsaturated metal centres for reactions such as oxidation to take place. A CdL₂-MOF was reported to display selective adsorption towards six analogous six-membered ring substrates under mild conditions, with selectivity in decreasing order: 1,4-dioxane > cyclohexane > cyclohexene and benzene > cyclohexanone > cyclohexanol.⁹¹ Another interesting feature of this

Cd(II)-MOF is its intense green-yellow luminescence when completely evacuated, which can enable it to be applied as a sensor for detecting the six organic substrates in the environment.

Chun *et al.*⁹² studied the adsorption capacity of three Group IV-MOFs derived from 2,5-dihydroxyterephthalic acid (H₄dobdc). The Ti(IV)-MOF, abbreviated as Ti-dobdc, was shown to exhibit relatively high isosteric heats of adsorption toward H₂ and CO₂ at 6.6 and 29.4 kJ mol⁻¹, signifying the reversible adsorption of these gases within the linear 1D channels within the pores of the MOF. On the other hand, the isostructural Zr- and Hf-dobdc MOFs, having a general formula of (H₃O)_x[M(dobdc)(bz)_x] (where bz = benzoate), possess a nonoxo-trinuclear building unit that gives rise to a 6-connected topology polyhedral network. The N₂ adsorption isotherms of Fe-porphyrin-MOFs were studied by Fateeva *et al.*⁹³, utilizing tetrakis(4-carboxyphenyl)porphyrin (H₂TCPP) as the ligand, yielding crystalline Fe-MOFs synthesized solvothermally under basic conditions. For the MOF MIL-141(Fe), a value of 0.19 cm³ g⁻¹ was obtained for its pore volume, and its BET surface area was measured, giving a good agreement between the experimental and calculated values of 420 and 468 m² g⁻¹, respectively. In addition, the second Fe(III)-MOF, Fe₂TCPP(FeOH)₂ (where pz = pyrazine), possesses a pore volume of 0.33 cm³ g⁻¹, and the value of the experimental BET surface area was measured to be lower – 760 m² g⁻¹ – than the calculated value of 1460 m² g⁻¹. For the Fe(II)-MOF, FeTCPP(Fe₂bpy)₂ (where bpy = 4,4'-bipyridine), a BET surface area of 900 m² g⁻¹ was obtained, which was, again, lower than the theoretical value (2900 m² g⁻¹). This discrepancy was attributed to a possible structural collapse upon activation.

An efficient methane and carbon dioxide adsorption capacity has been reported for the Al-MOFs known as MOF-519 and MOF-520,⁹⁴ and MOFs based on γ -cyclodextrin (CD-MOF-2).⁹⁵ The permanently porous MOF-519 and MOF-520 displayed excellent volumetric capacities towards carbon dioxide at 200 and 162 cm³ cm⁻³ at 35 bar,

273 K.⁹⁴ Enhanced capacities of 279 and 231 cm³ cm⁻³ for MOF-519 and MOF-520, respectively, were recorded at the same temperature but at a higher pressure (80 bar). Adsorption studies using the green CD-MOF-2 revealed its highly CO₂-selective nature even at low pressures.⁹⁵ In addition, this nanoporous MOF was shown to undergo reversible carbon fixation and decomposition even at room temperature, as indicated by solid-state ¹³C-NMR spectroscopy and colorimetric studies. The action of certain MOFs in aqueous media for adsorbing selectively harmful organic substances, such as dyes, aromatics from spilled oil, and herbicides, has also been documented by Hasan *et al.*⁹⁶

4.4 MOFs as antibacterial agents

Careful selection of the inorganic and organic building blocks can generate MOFs with high bactericidal activity as well as biocompatibility. Numerous MOFs have been studied for their antibacterial activities against various bacterial species, with many reports focusing on *E. coli* and *S. aureus*. Among these, the Ag(I)-MOFs have long been well known for their antibacterial activity, particularly the Ag(I)-carboxylate MOFs,⁹⁷ as has the role of their structure-activity relationship in their bioactivity.⁹⁸

The Ag(I)-MOFs [Ag₂(O-IPA)(H₂O)·H₃O] and [Ag₅(PYDC)₂(OH)] (where HO-H₂IPA = 5-hydroxyisophthalic acid and H₂PYDC = pyridine-3,5-dicarboxylic acid) exhibited excellent antibacterial activity with minimum inhibitory concentrations in the ranges 5-10 ppm and 10-15 ppm against *E. coli*, and 10-15 ppm and 15-20 ppm against *S. aureus*, respectively. Interestingly, the antibacterial activity of these MOFs is much improved over that of the Ag-nanoparticles. Based on their study, the authors concluded that the MOFs exerted their bactericidal effect by the release of Ag(I) ions, which then interact with thiol groups of proteins, resulting in overall bacterial disintegration.

Other transition metal-based MOFs, such as Co(II)- and Cu(II)-MOFs, also possess some level of antibacterial activity. For example, a Co(II)-MOF assembled from 4,4'-[benzene-1,4-

diylbis(methylylidenenitrilo)]dibenzoic acid (H₂bdda), Co₂(bdda)_{1.5}(OAc)·5H₂O, has been subject to antibacterial studies using the agar well diffusion method against *E. coli* and *B. cereus*.⁷⁸ This Co(II)-MOF was discovered to possess a slight antibacterial effect, with the diameters of the inhibition zones being 2.3 ± 1 cm and 3.5 ± 1 cm, respectively. Jo *et al.*⁹⁹ reported the synthesis of four glutarate-derived Cu(II)-MOFs based on different pyridyl derivatives – 4,4'-bipyridine (bpy), 1,2-bis(4-pyridyl)ethane (bpa), 1,2-bis(4-pyridyl)ethylene (bpe), and 1,2-bis(4-pyridyl)propane (bpp). Studies of their minimal bactericidal concentrations (MBCs) against *E. coli*, *S. aureus*, *K. pneumonia*, *P. aeruginosa*, and MRSA indicated that all four MOFs displayed 99.9% bactericidal effectiveness with MBCs of 20 µg ml⁻¹. As to the activity of each individual component of the MOFs, Cu(II) ions were the most active species, followed by bpe, bpp, glutarate, bpy, and bpa. The authors argued that the bactericidal property of the four Cu(II)-MOFs was controlled predominantly by physical properties such as the surface area, porosities, and size of the particles, rather than by the leaching of Cu(II) ions from the framework structure. These studies illustrate the richness, as well as the complex antibacterial mechanisms, associated with different MOF materials.

5. Conclusion

MOFs are a class of hybrid compounds that have numerous applications in various fields, such as in catalysis, as sensors, in gas adsorption and separation, and as potential antibacterial agents. A diverse array of crystal structures for these MOFs can be obtained by varying the functional groups or substituents incorporated in the organic ligands used, and they are partly affected also by the nature of the counterions present. While carboxylate-based ligands are commonly employed, Schiff bases and pyridyl-derived ligands are of equal importance in the crystal engineering of MOF structures for a wide scope of applications. Although the exploration of the potential of MOFs has been ongoing for more than two decades now, more in-depth studies are needed to fully explore the realm of possibilities that MOFs can offer.

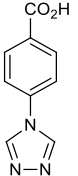
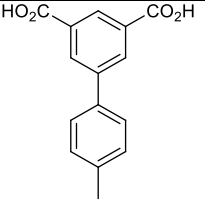
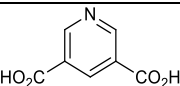
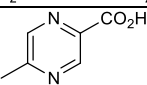
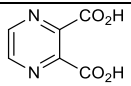
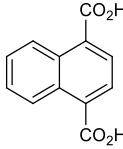
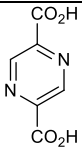
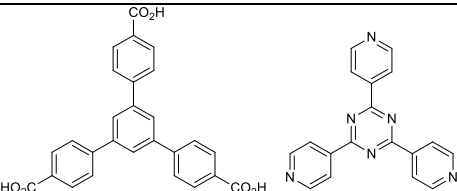
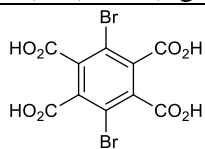
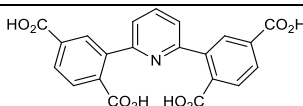
Conflict of interest

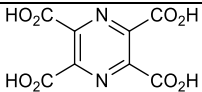
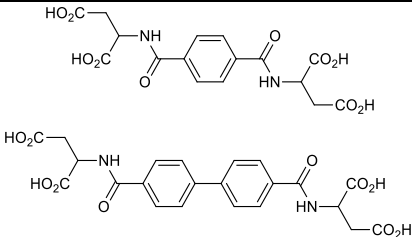
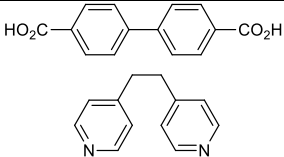
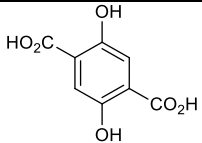
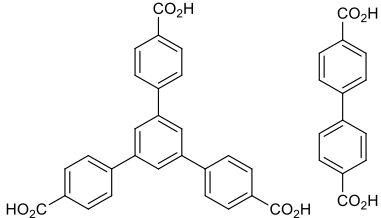
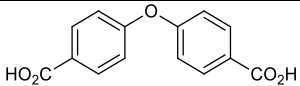
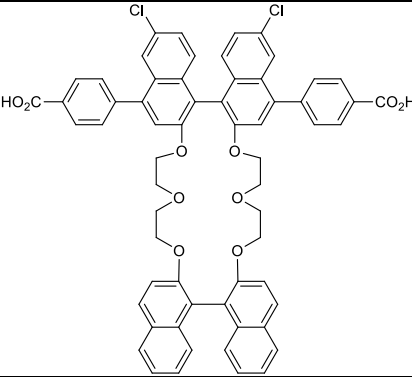
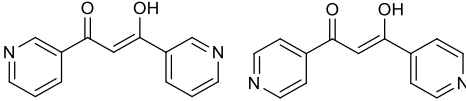
The authors have no conflicts of interest to declare.

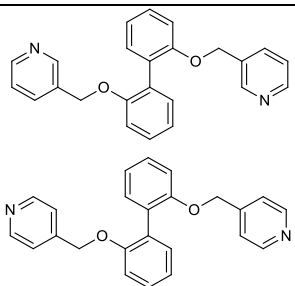
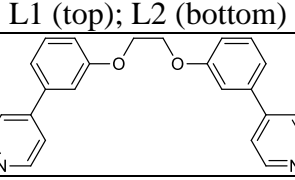
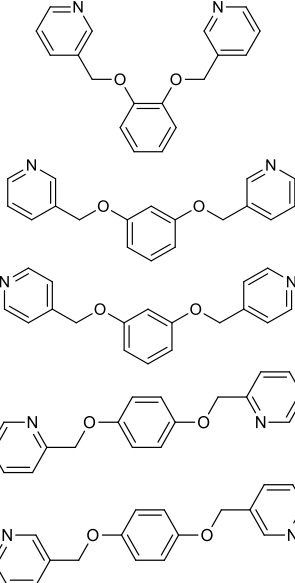
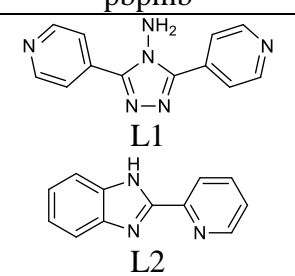
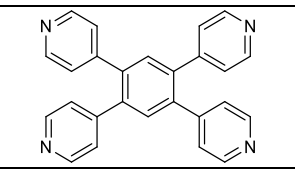
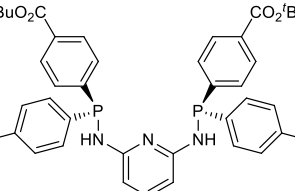
Acknowledgements

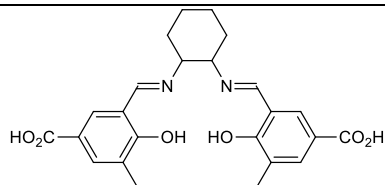
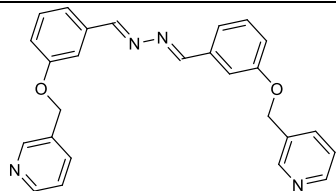
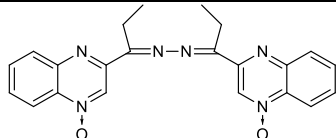
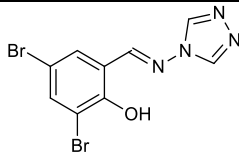
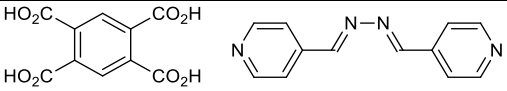
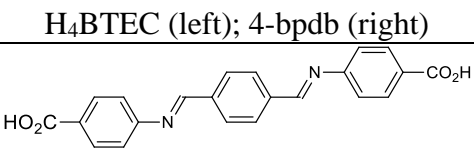
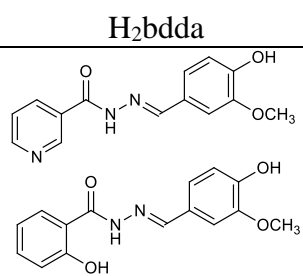
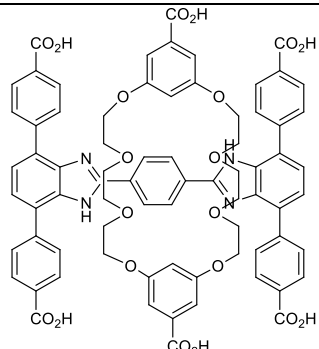
The work was supported by the Universiti Brunei Darussalam Graduate Scholarship.

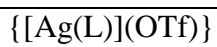
Table 1 Overview of organic ligands used in the construction of various MOFs.

MOF Formula	Metal ion	Ligand	Reference
Carboxylate derivatives			
$\{[\text{Ho}_8\text{Na}(\text{OH})_6\text{Cu}_{16}\text{I}_2(\text{L})_{24}](\text{NO}_3)_9(\text{H}_2\text{O})_6(\text{MeCN})_{18}\}_n$	Mixed metals		[29]
$\{[\text{Co}(\text{L})(\text{bpe})_{0.5}(\text{H}_2\text{O})]\cdot\text{H}_2\text{O}\}_n$ or $\{[\text{Co}(\text{L})(\text{bip})]\cdot 2\text{H}_2\text{O}\}_n$ (bpe = 1,2-bis(4-pyridyl)ethane; bip = 1,5-bis(imidazol)pentane)	Co^{II}		[30]
$[\text{Co}(\text{L})(\text{H}_2\text{O})_2]_n$ or $[\text{Co}(\text{L})(\text{H}_2\text{O})_4]_n(\text{H}_2\text{O})_n$	Co^{II}		[31]
$[\text{Ln}(\text{L})_2(\text{MeOH})_2\text{Ln}(\text{H}_2\text{O})_6\text{Mo}(\text{CN})_8]\cdot 8\text{H}_2\text{O}$ (Ln^{III} = Nd, Eu, Gd, Tb, or Er)	Ln^{III}		[32]
$[\text{UO}_2(\text{L})(\text{H}_2\text{O})_n]$ or $[(\text{UO}_2)_2\text{Cs}(\text{L})_2(\text{OH})(\text{H}_2\text{O})]$ ($n = 1, 2$)	UO_2^{2+}		[33]
$(\text{H}_3\text{O})_2[(\text{UO}_2)_2(\text{L})_3]\cdot\text{H}_2\text{O}$	UO_2^{2+}		[34]
$[\text{Zr}_6(\mu_3\text{-O})_4(\mu_3\text{-OH})_4(\mu\text{-OH})_2(\text{OH})_2(\text{H}_2\text{O})_2(\text{HCOO})_2(\text{L})_3]\cdot 10\text{H}_2\text{O}$	Zr^{IV}		[36]
$[\text{Cu}_2(\text{L}1)_2(\text{L}2)\text{Cl}]\cdot(\text{solvent})_x$ or $\{[\text{Ni}_3(\text{OH})(\text{L}2)_2(\text{L}1)[\text{NHMe}_2]]\}_n$	Cu^{II} or Ni^{II}		[37], [38]
$[\text{Ca}_2(\text{L})(\text{H}_2\text{O})_8]_n$ or $[\text{Ba}_2(\text{L})(\text{H}_2\text{O})_2]_n$	Ca^{II} or Ba^{II}		[39]
$[\text{Co}_3(\text{L})(\text{OH})_2(\text{H}_2\text{O})_4]\cdot\text{NMP}\cdot 3\text{H}_2\text{O}$ (NMP = 1-Methyl-2-pyrrolidinone)	Co^{II}		[40]

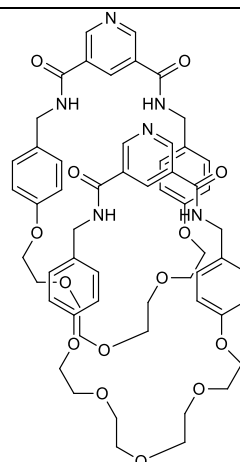
$[\text{K}_5\text{Ln}_5(\text{L})_5(\text{H}_2\text{O})_{19}] \cdot 7\text{H}_2\text{O}$ ($\text{Ln}^{\text{III}} = \text{Dy}, \text{Ho}, \text{or Yb}$)	$\text{K}^{\text{I}}\text{-Ln}^{\text{III}}$		[41]
$[\text{Na}_4(\text{L1})(\text{MeOH})(\text{H}_2\text{O})]$ or $[\text{Na}_4(\text{L2})(\text{H}_2\text{O})_2]$	Na^{I}		[42]
$[(\text{Fe}_3\text{O})_4(\text{SO}_4)_{12}(\text{BPDC})_6(\text{BPE})_6]^{8-}$ $\cdot 8[\text{NH}_2\text{Me}_2]^+ \cdot 13\text{H}_2\text{O} \cdot 8\text{DMF}$	Fe^{III}		[45]
$\text{Mg}_{0.269}\text{Ca}_{0.022}\text{Sr}_{0.030}\text{Ba}_{0.075}\text{Mn}_{0.234}\text{Fe}_{0.422}\text{Co}_{0.272}\text{Ni}_{0.282}\text{Zn}_{0.199}\text{Cd}_{0.196}(\text{DOT}) \cdot (\text{H}_2\text{O})_{7.8}$	Mixed transition metals		[46], [47]
$\text{Al}_8(\text{OH})_8(\text{BTB})_4(\text{BPDC})_2$	Al^{III}		[48]
$[\text{NaLn}(\text{L})(\text{ox})(\text{H}_2\text{O})]$ ($\text{Ln}^{\text{III}} = \text{Eu}, \text{or Sm}; \text{ox} = \text{oxalate}$)	$\text{Na}^{\text{I}}\text{-Ln}^{\text{III}}$		[54]
$[\text{Zn}_4\text{O}(\text{L})_3]$	Zn^{II}		[55]
Pyridyl and ether derivatives			
$[\text{AgFe}(\text{dppd})_3]\text{BF}_4 \cdot 2\text{DMSO} \cdot 2\text{H}_2\text{O}$ or $[\text{Ag}_2\text{Fe}(\text{dmppd})_3(\text{ONO}_2)]\text{NO}_3 \cdot \text{MeC N} \cdot \text{CH}_2\text{Cl}_2$	$\text{Ag}^{\text{I}}\text{-Fe}^{\text{III}}$		[49]

$[\text{Zn}_2(\text{L1})_2\text{Cl}_4]$ or $[\text{Zn}(\text{L2})\text{Cl}_2]_n$	Zn^{II}		[50]
$[\text{Cd}(\text{L})_2(\text{OTs})_2] \cdot 2(\text{solvent})$ (solvent = THF, PhF, PhBr)	Cd^{II}		[51]
$[\text{Cd}_2\text{Cl}_2(\text{L})(3\text{-obpmb})_2]_n$ $\{[\text{Cd}_2(\text{L})_2(3\text{-mbpmb})_3] \cdot 2.5\text{H}_2\text{O}\}_n$ $\{[\text{CdL}(4\text{-mbpmb})_2] \cdot \text{MeOH}\}_n$ $[\text{Cd}_2(\text{L})_2(2\text{-pbpmb})]_n$ $[\text{Cd}_2(\text{L})_2(3\text{-pbpmb})]_n$	Cd^{II}		[52], [53]
		(From top to bottom): 3-obpmb, 3-mbpmb, 4-mbpmb, 2-pbpmb, 3-pbpmb	
$[\text{Cd}(\text{SO}_4)(\text{L1})(\text{H}_2\text{O})]_n \cdot 3n\text{H}_2\text{O}$ or $[\text{Cd}(\text{D-cam})(\text{L2})(\text{H}_2\text{O})]_n$ (D-cam = D-camphorate)	Cd^{II}		[56]
$\{[\text{Ag}(\text{L})] \cdot \text{SbF}_6\}_n$	Ag^{I}		[57]
$[\text{Zr}_6\text{O}_4(\text{OH})_4(\text{OAc})_{2.4}\{(\text{P}^{\text{N}}\text{N}^{\text{N}}\text{P})\text{Pd}(\text{MeCN})\}_{2.4}(\text{BF}_4)_{2.4}$ ($\text{P}^{\text{N}}\text{N}^{\text{N}}\text{P}$ = 2,6-(HNPAr ₂) ₂ C ₅ H ₃ N; Ar = <i>p</i> -C ₆ H ₄ CO ₂ ⁻)	Zr^{IV}		[58]

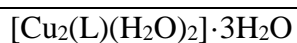
Schiff bases		
$[\text{BaNa}(\text{FeL})_2(\mu_2\text{-OH})(\text{H}_2\text{O})] \cdot \text{DMF} \cdot 2\text{H}_2\text{O}$	Mixed metals	 [73]
$\{[\text{Cd}(\text{L})(\text{SCN})_2] \cdot \text{CH}_2\text{Cl}_2\}_n$	Cd^{II}	 [74]
$\text{Ag}_3(\text{L})_2(\text{SbF}_6)_3 \cdot (\text{CHCl}_3) \cdot (\text{H}_2\text{O})$	Ag^{I}	 [75]
$[\text{M}(\text{L})_2]_n$ ($\text{M}^{\text{II}} = \text{Zn}, \text{Cd}$)	Zn^{II} or Cd^{II}	 [76]
$[\text{Co}_2(\text{BTEC})(4\text{-bpdb})(\text{H}_2\text{O})_2 \cdot 4\text{H}_2\text{O}]_n$	Co^{II}	 [77]
$\text{Co}_2(\text{bdda})_{1.5}(\text{OAc}) \cdot 5\text{H}_2\text{O}$	Co^{II}	 [78] H ₄ BTEC (left); 4-bpdb (right)
$[\text{Pb}_2(\text{L}_1)_2(\text{NO}_3)_2] \cdot 3\text{H}_2\text{O}$ or $[\text{Co}(\text{L}_2)_2(\text{py})_2] \cdot \text{ClO}_4$	Pb^{II} or Co^{III}	 [79] H ₂ bdda L ₁ (top); L ₂ (bottom)
Mechanically interlocked molecules		
$[\text{NH}_2\text{Me}_2]_2\{\text{Zn}_2\{\text{H}_2\text{O}\}_2(\text{L})\}$	Zn^{II}	 [25]



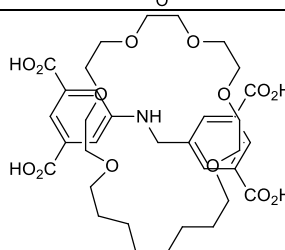
Ag^I



[26]



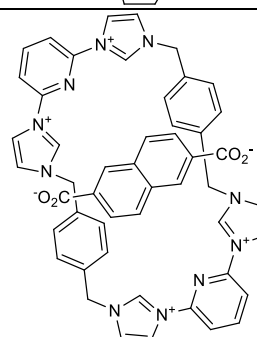
Cu^{II}



[27]

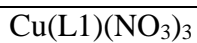


Ag^I or
Zn^{II}

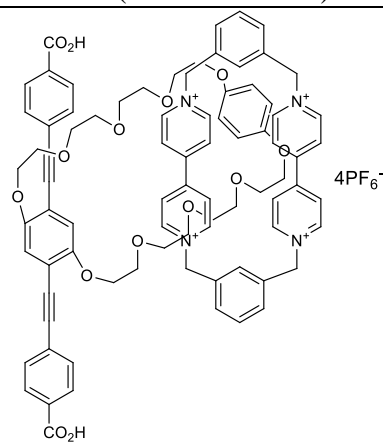


[80]

L = (NDC ⊂ TSMB)



Cu^{II}



[82]

H₂L1

Table 2. Overview of applications of some MOFs.

MOF formula	Description	Reference
IRMOF-3-SI-Au	Post synthetic modification-induced catalysis	[85]
Mo(acac) ₂ -UiO-66-NH ₂ MOF	Epoxidation of cyclic and aliphatic alkenes	[86]
Pd-pySal-Cu(BDC)	Mizoroki-Heck coupling reaction	[87]
Ln(4,4'-bipy)	Luminescence tuning by variation of Eu ^{III} /Tb ^{III} /Gd ^{III} ratio Presence of microporosity and mesoporosity (0.6-1.8 nm) BET surface area = 660 m ² g ⁻¹	[88]
Eu _{1.5} (L)	Exhibits intense red luminescence ($\phi = 73\%$)	[89]
[Cd(dpm) ₂]	First series of luminescent Cd-MOFs bearing mono-dpm ligands	[90]
Cd(L) ₂ -MOF	Selective adsorption of 6-membered ring substrates at mild conditions Exhibits intense green-yellow luminescence of evacuated MOF	[91]
(H ₃ O) _x (M(dobdc)(bz) _x) (M = Zr, Hf)	Reversible adsorption of H ₂ and CO ₂	[92]
FeTCPP(Febpy) ₂ and FepzTCPP(FeOH) ₂	Adsorption studies of N ₂ BET surface area = 900 and 760 m ² g ⁻¹	[93]
MOF-519 and MOF-520	Excellent CO ₂ volumetric capacities of 200 and 162 cm ³ cm ⁻³ at 273 K, 35 bar	[94]
CD-MOF-2	High selective adsorption of CO ₂ at low pressures Reversible carbon fixation and decomposition at room temperature	[95]
[Ag ₂ (O-IPA)(H ₂ O)·H ₃ O)] and [Ag ₅ (PYDC) ₂ (OH)]	Antibacterial active against <i>E. coli</i> and <i>S. aureus</i> with MIC values of 5-20 ppm	[97]
Co ₂ (bdda) _{1.5} (OAc)·5H ₂ O	Exhibits antibacterial property against <i>E. coli</i> and <i>B. cereus</i> with MIC values of 2.3 ± 1 cm and 3.5 ± 1 cm, respectively	[78]
[Cu ₂ (Glu) ₂ (X)]·nH ₂ O (X = bpy, bpa, bpe, bpp)	MBC value of 20 µg ml ⁻¹ against <i>E. coli</i> , <i>S. aureus</i> , <i>K. pneumonia</i> , <i>P. aeruginosa</i> and MRSA	[99]

References

- [1] O. M. Yaghi, G. Li, and H. Li, "Selective Binding and Removal of Guests in a Microporous Metal-Organic Framework," *Nature*, vol. 378, no. 6558, p. 703, 1995.
- [2] O. M. Yaghi and Q. Li, "Reticular Chemistry and Metal-Organic Frameworks for Clean Energy," *MRS Bull.*, vol. 34, no. 9, pp. 682-690, 2009.
- [3] Y. Dong, M. D. Smith, R. C. Layland, and H. Loye, "A Novel Noninterpenetrating Polycyclohexane Network: A New Inorganic/Organic Coordination Polymer Structural Motif Generated by Self-Assembly of 'T-Shaped' Moieties," *Chem. Mater.*, vol. 12, no. 4, pp. 1156-1161, 2000.
- [4] K. K. Gangu, S. Maddila, S. B. Mukkamala, and S. B. Jonnalagadda, "A Review on Contemporary Metal-Organic Framework Materials," *Inorganica Chim. Acta*, vol. 446, pp. 61-74, 2016.
- [5] I. Imaz and D. Maspoch, "Self-Assembly of Coordination Chains and Helices," in *Supramolecular Chemistry: From Molecules to Nanomaterials*, 1st ed., vol. 5, P. A. Gale and J. W. Steed, Eds. West Sussex: John Wiley & Sons, Ltd, 2012, pp. 2045-2069.

- [6] N. Stock and S. Biswas, "Synthesis of Metal-Organic Frameworks (MOFs): Routes to Various MOF Topologies, Morphologies, and Composites," *Chem. Rev.*, vol. 112, no. 2, pp. 933-969, 2012.
- [7] D. J. Tranchemontagne, J. R. Hunt, and O. M. Yaghi, "Room Temperature Synthesis of Metal-Organic Frameworks: MOF-5, MOF-74, MOF-177, MOF-199, and IRMOF-0," *Tetrahedron*, vol. 64, pp. 8553-8557, 2008.
- [8] G. G. da Silva, F. L. A. Machado, S. A. Junior, and E. Padrón-Hernández, "Metal-Organic Framework: Structure and Magnetic Properties of $[\text{Cu}_3(\text{BTC})_2(\text{L})_x(\text{CuO})_y]_n$ ($\text{L}=\text{H}_2\text{O}$, DMF)," *J. Solid State Chem.*, vol. 253, pp. 1-5, Sep. 2017.
- [9] J. I. Feldblyum, M. Liu, D. W. Gidley, and A. J. Matzger, "Reconciling the discrepancies between crystallographic porosity and guest access as exemplified by Zn-HKUST-1," *J. Am. Chem. Soc.*, vol. 133, no. 45, pp. 18257-18263, Nov. 2011.
- [10] Y. R. Lee, J. Kim, and W. S. Ahn, "Synthesis of Metal-Organic Frameworks: A Mini Review," *Korean J. Chem. Eng.*, vol. 30, no. 9, pp. 1667-1680, 2013.
- [11] R. González-Prieto, S. Herrero, R. Jiménez-Aparicio, and 4 others, "Microwave-Assisted Solvothermal Synthesis of Inorganic Compounds (Molecular and Non Molecular)," *Microw. Chem.*, no. February 2018, pp. 225-247, 2017.
- [12] D. Chen, J. Zhao, P. Zhang, and S. Dai, "Mechanochemical Synthesis of Metal-Organic Frameworks," *Polyhedron*, vol. 162, pp. 59-64, 2019.
- [13] A. Pichon, A. Lazuen-Garay, and S. L. James, "Solvent-Free Synthesis of a Mmicroporous Metal-Organic Framework," *CrystEngComm*, vol. 8, no. 3, pp. 211-214, 2006.
- [14] M. G. Campbell, D. Sheberla, S. F. Liu, T. M. Swager, and M. Dincă, "Cu₃(hexaiminotriphenylene)₂: An Electrically Conductive 2D Metal-Organic Framework for Chemiresistive Sensing," *Angew. Chemie - Int. Ed.*, vol. 54, no. 14, pp. 4349-4352, 2015.
- [15] C.-S. Liu, Z. Chang, J.-J. Wang, L.-F. Yan, X.-H. Bu, and S. R. Batten, "A Photoluminescent 3D Silver(I) Coordination Polymer with Mixed Ligands Anthracene-9,10-dicarboxylate and Hexamethylenetetramine, Showing Binodal 4-Connected (43·63)₂(42·62·82)₃ Topology," *Inorg. Chem. Commun.*, vol. 11, no. 8, pp. 889-892, Aug. 2008.
- [16] D. Sheberla, L. Sun, M. Blood-Forsythe and 5 others, "High Electrical Conductivity in Ni₃(2,3,6,7,10,11-hexaiminotriphenylene)₂, a Semiconducting Metal-Organic Graphene Analogue," *J. Am. Chem. Soc.*, vol. 136, pp. 8859-8862, 2014.
- [17] F.-L. Liu, Z.-H. Xu, X.-Y. Zhang, X.-P. Wang, and D. Sun, "Unusual N-H Activation of 2-Aminopyrimidine: Supramolecular Assembly into an AgI Metal-Organic Framework," *Chem. - An Asian J.*, vol. 9, no. 2, pp. 452-456, Feb. 2014.
- [18] P. Li, S. Regati, H. C. Huang, H. D. Arman, B. L. Chen, and J. C. G. Zhao, "A Sulfonate-Based Cu(I) Metal-Organic Framework as a Highly Efficient and Reusable Catalyst for the Synthesis of Propargylamines Under Solvent-Free Conditions," *Chinese Chem. Lett.*, vol. 26, no. 1, pp. 6-10, 2015.
- [19] X. L. Zhang, G. M. Tang, and Y. T. Wang, "Tunable Luminescent Behaviors of Ag-Containing Metal Coordination Polymers with N-Heterocyclic and Sulfonate Group," *Polyhedron*, vol. 147, pp. 26-35, 2018.
- [20] X. L. Zhang, G. M. Tang, and Y. T. Wang, "A Set of Ag-Based Metal Coordination Polymers with Sulfonate Group: Syntheses, Crystal Structures and Luminescent Behaviors," *Polyhedron*, vol. 148, pp. 55-69, 2018.
- [21] M. Bazaga-García, R. M. P. Colodrero, M. Papadaki and 9 others, "Guest Molecule-Responsive Functional Calcium Phosphonate Frameworks for Tuned Proton Conductivity," *J. Am. Chem. Soc.*, vol. 136, no. 15, pp. 5731-5739, 2014.
- [22] P. Deria, W. Bury, I. Hod and 4 others,

- “MOF Functionalization via Solvent-Assisted Ligand Incorporation: Phosphonates vs Carboxylates,” *Inorg. Chem.*, vol. 54, no. 5, pp. 2185-2192, 2015.
- [23] Z. H. Fard, Y. Kalinovsky, D. M. Spasyuk, B. A. Blight, and G. K. H. Shimizu, “Alkaline-Earth Phosphonate MOFs with Reversible Hydration-Dependent Fluorescence,” *Chem. Commun.*, vol. 52, no. 87, pp. 12865-12868, 2016.
- [24] K. J. Gagnon, H. P. Perry, and A. Clearfield, “Conventional and Unconventional Metal-Organic Frameworks Based on Phosphonate Ligands: MOFs and UMOFs,” *Chem. Rev.*, vol. 112, no. 2, pp. 1034-1054, 2012.
- [25] G. Gholami, K. Zhu, J. S. Ward, P. E. Kruger, and S. J. Loeb, “Formation of a Polythreaded, Metal-Organic Framework Utilizing an Interlocked Hexadentate, Carboxylate Linker,” *Eur. J. Inorg. Chem.*, vol. 2016, no. 27, pp. 4524-4529, 2016.
- [26] J. E. M. Lewis, “Self-Templated Synthesis of Amide Catenanes and Formation of a Catenane Coordination Polymer,” *Org. Biomol. Chem.*, vol. 17, no. 9, pp. 2442-2447, 2019.
- [27] V. N. Vukotic, K. J. Harris, K. Zhu, R. W. Schurko, and S. J. Loeb, “Metal-Organic Frameworks with Dynamic Interlocked Components,” *Nat. Chem.*, vol. 4, no. 6, pp. 456-460, 2012.
- [28] S. Yuan, L. Feng, K. Wang and 14 others, “Stable Metal-Organic Frameworks: Design, Synthesis, and Applications,” *Adv. Mater.*, vol. 30, no. 37, p. 1704303, Sep. 2018.
- [29] M. Zhao, S. Chen, Y. Huang, and Y. Dan, “An Unusual 2p-3d-4f Heterometallic Coordination Polymer Featuring Ln₈Na and Cu₈I Clusters as Nodes,” *J. Mol. Struct.*, vol. 1128, pp. 123-126, 2017.
- [30] X.-H. Chang, L.-F. Ma, G. Hui, and L.-Y. Wang, “Four Low-Dimensional Cobalt(II) Coordination Polymers Based on a New Isophthalic Acid Derivative: Syntheses, Crystal Structures, and Properties,” *Cryst. Growth Des.*, vol. 12, no. 7, pp. 3638-3646, Jul. 2012.
- [31] A. Cheansirisomboon, C. Pakawatchai, and S. Youngme, “2D-1D Structural Phase Transformation of Co(II) 3,5-Pyridinedicarboxylate Frameworks with Chromotropism,” *Dalt. Trans.*, vol. 41, no. 35, pp. 10698-10706, Aug. 2012.
- [32] S. Tanase, M. C. Mittelmeijer-Hazeleger, G. Rothenberg and 4 others, “A Facile Building-Block Synthesis of Multifunctional Lanthanide MOFs,” *J. Mater. Chem.*, vol. 21, no. 39, pp. 15544-15551, Sep. 2011.
- [33] B. Masci and P. Thuéry, “Hydrothermal Synthesis of Uranyl-Organic Frameworks with Pyrazine-2,3-dicarboxylate Linkers,” *CrystEngComm*, vol. 10, no. 8, pp. 1082-1087, Jul. 2008.
- [34] W. Xu, Y.-N. Ren, M. Xie, L.-X. Zhou, and Y.-Q. Zheng, “Six Uranyl-Organic Frameworks with Naphthalene-Dicarboxylic Acid and Bipyridyl-Based Spacers: Syntheses, Structures, and Properties,” *Dalt. Trans.*, vol. 47, no. 12, pp. 4236-4250, Mar. 2018.
- [35] J.-N. Rebilly, J. Bacsá, and M. J. Rosseinsky, “1D Tubular and 2D Metal-Organic Frameworks Based on a Flexible Amino Acid Derived Organic Spacer,” *Chem. - An Asian J.*, vol. 4, no. 6, pp. 892-903, Jun. 2009.
- [36] S. Waitschat, H. Reinsch, and N. Stock, “Water-Based Synthesis and Characterisation of a New Zr-MOF with a Unique Inorganic Building Unit,” *Chem. Commun.*, vol. 52, no. 86, pp. 12698-12701, 2016.
- [37] A. Nath, S. Das, P. Mukharjee, R. Nath, D. Kuznetsov, and S. Mandal, “Frustrated Magnetism in Cu(II) Based Metal-Organic Framework,” *Inorganica Chim. Acta*, vol. 486, no. August 2018, pp. 158-161, 2019.
- [38] J. Y. Tan, J. X. Shi, P. H. Cui and 4 others, “A Ni₃(OH)(COO)₆-Based MOF from C₃ Symmetric Ligands: Structure and Heterogeneous Catalytic Activities in One-Pot Synthesis of Imine,” *Microporous Mesoporous Mater.*, vol. 287, no. March, pp. 152-158, 2019.

- [39] S. Du, C. Ji, X. Xin and 5 others, "Syntheses, Structures and Characteristics of Four Alkaline-Earth Metal-Organic Frameworks (MOFs) Based on Benzene-1,2,4,5-tetracarboxylic Acid and Its Derivative Ligand," *J. Mol. Struct.*, vol. 1130, pp. 565-572, Feb. 2017.
- [40] Y. Wu, S. Cheng, J. Liu, G. Yang, and Y. Y. Wang, "New Porous Co(II)-Based Metal-Organic Framework including 1D Ferromagnetic Chains with Highly Selective Gas Adsorption and Slow Magnetic Relaxation," *J. Solid State Chem.*, vol. 276, no. May, pp. 226-231, 2019.
- [41] F. Zhang, P. Yan, X. Zou, J. Zhang, G. Hou, and G. Li, "Novel 3D Alkali-Lanthanide Heterometal-Organic Frameworks with Pyrazine-2,3,5,6-tetracarboxylic Acid: Synthesis, Structure, and Magnetism," *Cryst. Growth Des.*, vol. 14, no. 4, pp. 2014-2021, Apr. 2014.
- [42] P. Siman, C. A. Trickett, H. Furukawa, and O. M. Yaghi, "1-Aspartate Links for Stable Sodium Metal-Organic Frameworks," *Chem. Commun.*, vol. 51, no. 98, pp. 17463-17466, Nov. 2015.
- [43] I. Imaz, M. Rubio-Martínez, J. An, I. Sole-Font, N. L. Rosi, and D. Maspoch, "Metal-Biomolecule Frameworks (MBioFs)," *Chem. Commun.*, vol. 47, no. 26, pp. 7287-7302, 2011.
- [44] M. Eddaoudi, D. B. Moler, H. Li and 4 others, "Modular Chemistry: Secondary Building Units as a Basis for the Design of Highly Porous and Robust Metal-Organic Carboxylate Frameworks," *Acc. Chem. Res.*, vol. 34, no. 4, pp. 319-330, 2001.
- [45] A. C. Sudik, A. P. Côte, A. G. Wong-foy, M. O. Keeffe, and O. M. Yaghi, "A Metal-Organic Framework with a Hierarchical System of Pores and Tetrahedral Building Blocks," *Angew. Chemie Int. Ed.*, vol. 45, no. 16, pp. 2528-2533, 2006.
- [46] H. Deng, S. Grunder, K. E. Cordova and 12 others, "Large-Pore Apertures in a Series of Metal-Organic Frameworks," *Science (80-.)*, vol. 336, no. 6084, pp. 1018-1023, 2012.
- [47] L. J. Wang, H. Deng, H. Furukawa and 4 others, "Synthesis and Characterization of Metal-Organic Framework-74 Containing 2, 4, 6, 8, and 10 Different Metals," *Inorg. Chem.*, vol. 53, no. 12, pp. 5881-5883, 2014.
- [48] E. A. Kapustin, S. Lee, A. S. Alshammari, and O. M. Yaghi, "Molecular Retrofitting Adapts a Metal-Organic Framework to Extreme Pressure," *ACS Cent. Sci.*, vol. 3, no. 6, pp. 662-667, 2017.
- [49] A. D. Burrows, M. F. Mahon, C. L. Renouf, C. Richardson, A. J. Warren, and J. E. Warren, "Dipyridyl β -Diketonate Complexes and Their Use as Metalloligands in the Formation of Mixed-Metal Coordination Networks," *Dalt. Trans.*, vol. 41, no. 14, pp. 4153-4163, 2012.
- [50] R. Wang, L. Han, L. Xu and 4 others, "Syntheses and Characterizations of Metal-Organic Frameworks with Unusual Topologies Derived from Flexible Dipyridyl Ligands," *Eur. J. Inorg. Chem.*, vol. 2004, no. 18, pp. 3751-3763, 2004.
- [51] L. Wang, Y. Li, F. Yang, Q. Liu, and Y. Dong, "Cd(II)-MOF: Adsorption, Separation, and Guest-Dependent Luminescence for Monohalobenzenes," *Inorg. Chem.*, vol. 53, no. 17, pp. 9087-9094, 2014.
- [52] L. Liu, C. Yu, F. Ma and 4 others, "Structural Diversity and Photocatalytic Properties of Cd (II) Coordination Polymers Constructed by a Flexible V-Shaped Bipyridyl Benzene Ligand and Dicarboxylate Derivatives," *Dalt. Trans.*, vol. 44, no. 4, pp. 1636-1645, 2015.
- [53] L. L. Liu, C. X. Yu, Y. R. Li, J. J. Han, F. J. Ma, and L. F. Ma, "Positional Isomeric Effect on the Structural Variation of Cd (II) Coordination Polymers Based on Flexible Linear/V-Shaped Bipyridyl Benzene Ligands," *CrystEngComm*, vol. 17, no. 3, pp. 653-664, 2015.
- [54] C. Wang, G. Guo, and P. Wang, "Two Sodium and Lanthanide(III) MOFs Based on Oxalate and V-Shaped 4,4'-Oxybis(benzoate) Ligands: Hydrothermal Synthesis, Crystal Structure, and

- Luminescence Properties,” *J. Mol. Struct.*, vol. 1032, pp. 93-99, Jan. 2013.
- [55] C. Valente, E. Choi, M. E. Belowich and 6 others, “Metal-Organic Frameworks with Designed Chiral Recognition Sites,” *Chem. Commun.*, vol. 46, no. 27, pp. 4911-4913, 2010.
- [56] N. Chen, M. X. Li, P. Yang, X. He, M. Shao, and S. R. Zhu, “Chiral Coordination Polymers with SHG-Active and Luminescence: An Unusual Homochiral 3D MOF Constructed from Achiral Components,” *Cryst. Growth Des.*, vol. 13, no. 6, pp. 2650-2660, 2013.
- [57] Y. Sun and H. Han, “A Novel 3D AgI Cationic Metal-Organic Framework Based on 1,2,4,5-Tetra(4-pyridyl)benzene with Selective Adsorption of CO₂ over CH₄, H₂O over C₂H₅OH, and Trapping Cr₂O₇²⁻,” *J. Mol. Struct.*, vol. 1194, pp. 73-77, 2019.
- [58] B. R. Reiner, A. A. Kassie, and C. R. Wade, “Unveiling Reactive Metal Sites in a Pd Pincer MOF: Insights into Lewis Acid and Pore Selective Catalysis,” *Dalt. Trans.*, vol. 48, no. 26, pp. 9588-9595, 2019.
- [59] N. E. Borisova, M. D. Reshetova, and Y. A. Ustynyuk, “Metal-free methods in the synthesis of macrocyclic Schiff bases,” *Chem. Rev.*, vol. 107, no. 1, pp. 46-79, 2007.
- [60] W. Al Zoubi, “Biological Activities of Schiff Bases and Their Complexes: A Review of Recent Works,” *Int. J. Org. Chem.*, vol. 03, no. 03, pp. 73-95, 2013.
- [61] D. Dragancea, A. W. Addison, M. Zeller and 4 others, “Dinuclear Copper(II) Complexes with Bis-Thiocarbohydrazone Ligands,” *Eur. J. Inorg. Chem.*, vol. 2008, no. 16, pp. 2530-2536, 2008.
- [62] V. Stilinović, D. Cinčić, M. Zbačnik, and B. Kaitner, “Controlling Solvate Formation of a Schiff Base by Combining Mechanochemistry with Solution Synthesis,” *Croat. Chem. Acta*, vol. 85, no. 4, pp. 485-493, 2012.
- [63] S. Chigurupati, S. Muralidharan, L. S. Cin, W. Y. Raser, K. Santhi, and K. S. Kesavanarayanan, “Studying Newly Synthesized and Developed 4-Hydroxy-3-Methoxybenzaldehyde Schiff Bases by UV Spectrophotometry and High Performance Liquid Chromatography,” *Pharm. Chem. J.*, vol. 50, no. 12, pp. 851-856, 2017.
- [64] D. H. Jornada, G. F. Dos Santos Fernandes, D. E. Chiba, T. R. F. De Melo, J. L. Dos Santos, and M. C. Chung, “The Prodrug Approach: A Successful Tool for Improving Drug Solubility,” *Molecules*, vol. 21, no. 1, p. 42, 2016.
- [65] S. Prasad and K. Susila, “An Overview on Schiff Bases and Its Medicinal Chemistry Potential for New Antitubercular Drug Molecules Research,” *Rev. Roum. Chim.*, vol. 62, no. 1, pp. 65-79, 2017.
- [66] K. H. M. E. Tehrani, S. Sardari, V. Mashayekhi, M. Esfahani Zadeh, P. Azerang, and F. Kobarfard, “One Pot Synthesis and Biological Activity Evaluation of Novel Schiff Bases Derived from 2-Hydrazinyl-1,3,4-thiadiazole,” *Chem. Pharm. Bull. (Tokyo)*, vol. 61, no. 2, pp. 160-166, 2013.
- [67] C. Vartzouma, E. Evaggellou, Y. Sanakis, N. Hadjiliadis, and M. Louloudi, “Alkene Epoxidation by Homogeneous and Heterogenised Manganese(II) Catalysts with Hydrogen Peroxide,” *J. Mol. Catal. A Chem.*, vol. 263, no. 1-2, pp. 77-85, 2007.
- [68] B. K. Momidi, V. Tekuri, and D. R. Trivedi, “Multi-Signaling Thiocarbohydrazone Based Colorimetric Sensors for the Selective Recognition of Heavy Metal Ions in an Aqueous Medium,” *Spectrochim. Acta Part A Mol. Biomol. Spectrosc.*, vol. 180, pp. 175-182, 2017.
- [69] C. Biswas, M. G. B. Drew, and A. Ghosh, “Stabilization of a Helical Water Chain in a Metal-Organic Host of a Trinuclear Schiff Base Complex,” *Inorg. Chem.*, vol. 47, no. 11, pp. 4513-4519, 2008.
- [70] B. T. Thaker, P. Patel, A. D. Vansadia, and H. G. Patel, “Synthesis, Characterization, and Mesomorphic Properties of New Liquid-Crystalline Compounds Involving Ester-Azomethine Central Linkages, Lateral Substitution, and a Thiazole Ring,” *Mol. Cryst. Liq. Cryst.*, vol. 466, no. 1, pp.

- 13-22, 2007.
- [71] M. Zbačnik, I. Nogalo, D. Cinčić, and B. Kaitner, "Polymorphism Control in the Mechanochemical and Solution-Based Synthesis of a Thermochromic Schiff Base," *CrystEngComm*, vol. 17, no. 41, pp. 7870-7877, 2015.
- [72] M. Zbačnik, K. Pičuljan, J. Parlov-Vuković, P. Novak, and A. Roodt, "Four Thermochromic o-Hydroxy Schiff Bases of α -Aminodiphenylmethane: Solution and Solid State Study," *Crystals*, 2017.
- [73] H. H. Wang, J. Yang, Y. Y. Liu, S. Song, and J. F. Ma, "Heterotrimetallic Organic Framework Assembled with FeIII/BaII/NaI and Schiff Base: Structure and Visible Photocatalytic Degradation of Chlorophenols," *Cryst. Growth Des.*, vol. 15, no. 10, pp. 4986-4992, 2015.
- [74] J. Xiao, C. Chen, Q. Liu, J. Ma, and Y. Dong, "Cd (II)-Schiff-Base Metal-Organic Frameworks: Synthesis, Structure, and Reversible Adsorption and Separation of Volatile Chlorocarbons," *Cryst. Growth Des.*, vol. 11, no. 12, pp. 5696-5701, 2011.
- [75] J. Y. Cheng, P. Wang, J. P. Ma, Q. K. Liu, and Y. B. Dong, "A Nanoporous Ag (I)-MOF Showing Unique Selective Adsorption of Benzene Among its Organic Analogues," *Chem. Commun.*, vol. 50, no. 89, pp. 13672-13675, 2014.
- [76] S. Zhang, J. Wang, H. Zhang, Y. Fan, and Y. Xiao, "Highly Efficient Electrochemiluminescence Based on 4-Amino-1,2,4-triazole Schiff Base Two-Dimensional Zn/Cd Coordination Polymers," *Dalt. Trans.*, vol. 46, no. 2, pp. 410-419, 2017.
- [77] Q. Sun, X. Zhu, N. Zhang, B. Zhang, J. Lu, and H. Liu, "Auxiliary Ligand-Assisted Structural Variation of Two Co (II) Metal-Organic Frameworks: Syntheses, Crystal Structure and Magnetic Properties," *Inorg. Chem. Commun.*, vol. 99, pp. 172-175, 2019.
- [78] S. Aryanejad, G. Bagherzade, and M. Moudi, "Design and Development of Novel Co - MOF Nanostructures as an Excellent Catalyst for Alcohol Oxidation and Henry Reaction, with a Potential Antibacterial Activity," *Appl. Organomet. Chem.*, vol. 33, no. 9, p. e4820, 2019.
- [79] S. Li, S. Gao, S. Liu, and Y. Guo, "Five Metal (II) Coordination Polymers Constructed from Two Vanillin Derivatives: From Discrete Structure to 3D Diamondoid Network," *Cryst. Growth Des.*, vol. 10, no. 2, pp. 495-503, 2010.
- [80] K. Zhu and S. J. Loeb, "Organizing Mechanically Interlocked Molecules to Function Inside Metal-Organic Frameworks," in *Top Current Chemistry*, no. 0000, Springer, 2014, pp. 1-39.
- [81] Q. Li, C.-H. Sue, S. Basu and 7 others, "A Catenated Strut in a Catenated Metal-Organic Framework," *Angew. Chemie Int. Ed.*, vol. 49, no. 38, pp. 6751-6755, 2010.
- [82] Q. Li, W. Zhang, S. Ognjen, J. F. Stoddart, and O. M. Yaghi, "A Metal-Organic Framework Replete with Ordered Donor-Acceptor Catenanes," *Chem. Commun.*, vol. 46, no. 3, pp. 380-382, 2010.
- [83] S. Zhang, Q. Yang, X. Liu and 5 others, "High-Energy Metal-Organic Frameworks (HE-MOFs): Synthesis, Structure and Energetic Performance," *Coord. Chem. Rev.*, vol. 307, pp. 292-312, Jan. 2016.
- [84] J. Jiang and O. M. Yaghi, "Brønsted Acidity in Metal-Organic Frameworks," *Chem. Rev.*, vol. 115, no. 14, pp. 6966-6997, Jul. 2015.
- [85] X. Zhang, F. X. L. Xamena, and A. Corma, "Gold (III)-Metal Organic Framework Bridges the Gap Between Homogeneous and Heterogeneous Gold Catalysts," *J. Catal.*, vol. 265, no. 2, pp. 155-160, 2009.
- [86] R. Kardanpour, S. Tangestaninejad, V. Mirkhani, M. Moghadam, I. Mohammadpoor-Baltork, and F. Zadehahmadi, "Efficient Alkene Epoxidation Catalyzed by Molybdenyl Acetylacetonate Supported on Aminated UiO-66 Metal-Organic Framework," *J. Solid State Chem.*, vol. 226, pp. 262-272, 2015.
- [87] H. Alamgholiloo, S. Rostamnia, A. Hassankhani and 4 others, "Stepwise Post-Modification Immobilization of Palladium

- Schiff- Base Complex on to the OMS- Cu (BDC) Metal-Organic Framework for Mizoroki- Heck Cross- Coupling Reaction,” *Appl. Organomet. Chem.*, vol. 32, no. 11, p. e4539, 2018.
- [88] P. R. Matthes, C. J. Höller, M. Mai and 6 others, “Luminescence Tuning of MOFs via Ligand to Metal and Metal to Metal Energy Transfer by Co-Doping of 2∞ [Gd 2 Cl 6 (bipy) 3]· 2bipy with Europium and Erbium,” *J. Mater. Chem.*, vol. 22, no. 20, pp. 10179-10187, 2012.
- [89] A. Duerrbeck, S. Gorelik, J. Hobley, A. Hor, and N. Long, “Highly Emissive, Solution-Processable and Dynamic Eu (III)-Containing Coordination Polymers,” *Chem. Commun.*, vol. 41, no. 41, pp. 8656-8659, 2015.
- [90] A. Béziau, S. A. Baudron, A. Guenet, and M. W. Hosseini, “Luminescent Coordination Polymers Based on Self-Assembled Cadmium Dipyrrin Complexes,” *Chem. Eur. J.*, vol. 19, no. 9, pp. 3215-3223, 2013.
- [91] L. Duan, Z. Wu, J. Ma, X. Wu, and Y. Dong, “Adsorption and Separation of Organic Six-Membered Ring Analogues on Neutral Cd (II) -MOF Generated from Asymmetric Schiff-Base Ligand,” *Inorg. Chem.*, vol. 49, no. 23, pp. 11164-11173, 2010.
- [92] H. Chun and D. Moon, “Metal–Organic Frameworks from Group 4 Metals and 2,5-Dihydroxyterephthalic Acid: Reinvestigation, New Structure, and Challenges Toward Gas Storage and Separation,” *Cryst. Growth Des.*, vol. 17, no. 4, pp. 2140-2146, 2017.
- [93] A. Fateeva, J. Clarisse, G. Pilet and 9 others, “Iron and Porphyrin Metal–Organic Frameworks: Insight into Structural Diversity, Stability, and Porosity,” *Cryst. Growth Des.*, vol. 15, no. 4, pp. 1819-1826, 2015.
- [94] F. Gándara, H. Furukawa, S. Lee, and O. M. Yaghi, “High Methane Storage Capacity in Aluminum Metal-Organic Frameworks,” *J. Am. Chem. Soc.*, vol. 136, no. 14, pp. 5271-5274, Apr. 2014.
- [95] J. J. Gassensmith, H. Furukawa, R. A. Smaldone and 4 others, “Strong and Reversible Binding of Carbon Dioxide in a Green Metal-Organic Framework,” *J. Am. Chem. Soc.*, vol. 133, no. 39, pp. 15312-15315, Oct. 2011.
- [96] Z. Hasan and S. H. Jung, “Removal of Hazardous Organics from Water Using Metal-Organic Frameworks (MOFs): Plausible Mechanisms for Selective Adsorptions,” *J. Hazard. Mater.*, vol. 283, pp. 329-339, Feb. 2015.
- [97] X. Lu, J. Ye, D. Zhang and 6 others, “Silver Carboxylate Metal-Organic Frameworks with Highly Antibacterial Activity and Biocompatibility,” *J. Inorg. Biochem.*, vol. 138, pp. 114-121, Sep. 2014.
- [98] R. Karimi Alavijeh, S. Beheshti, K. Akhbari, and A. Morsali, “Investigation of Reasons for Metal-Organic Framework’s Antibacterial Activities,” *Polyhedron*, vol. 156, pp. 257-278, Dec. 2018.
- [99] J. H. Jo, H. C. Kim, S. Huh, Y. Kim, and D. N. Lee, “Antibacterial Activities of Cu-MOFs Containing Glutarates and Bipyridyl Ligands,” *Dalt. Trans.*, vol. 48, no. 23, pp. 8084-8093, 2019.